RSC Advances

This article can be cited before page numbers have been issued, to do this please use: M. Brindisi, S. Brogi, S. Maramai, A. Grillo, G. Borrelli, S. Butini, E. Novellino, M. Allara, A. Ligresti, G. Campiani, V. Di Marzo and S. Gemma, *RSC Adv.*, 2016, DOI: 10.1039/C6RA12524G.

View Article Online
DOI: 10.1039/C6RA12524G

Journal Name

ARTICLE

Received 00th January 20xx,

Accepted 00th January 20xx

DOI: 10.1039/x0xx00000x

www.rsc.org/

Harnessing the pyrroloquinoxaline scaffold for FAAH and MAGL interaction: definition of the structural determinants for enzyme inhibition

Margherita Brindisi,[a,b] Simone Brogi,[a,b] Samuele Maramai,[a,b] Alessandro Grillo,[a,b] Giuseppe Borrelli,[a,b] Stefania Butini,[a,b,*] Ettore Novellino,[a,c] Marco Allarà,[d] Alessia Ligresti,[d] Giuseppe Campiani,[a,b,*] Vincenzo Di Marzo,[d] Sandra Gemma[a,b]

This paper describes the development of piperazine and 4-aminopiperidine carboxamides/carbamates supported on a pharmacogenic pyrroloquinoxaline scaffold as inhibitors of the endocannabinoid catabolizing enzymes fatty acid amide hydrolase (FAAH) and monoacylglycerol lipase (MAGL). Structure–activity relationships and molecular modelling studies allowed the definition of the structural requirements for dual FAAH/MAGL inhibition and led to the identification of a small set of derivatives (compounds **5e,i,k,m**) displaying a balanced inhibitory profile against both enzymes, with compounds **5m** being the frontrunner of the subset. Favorable calculated physico-chemical properties suggest further investigation for specific analogues.

Introduction

Endocannabinoids (ECs) *N*-arachidonoylethanolamine (AEA) and 2-arachidonoylglycerol (2-AG) stimulate cannabinoid CB1 and CB2 receptors (CB1R and CB2R)[1] thus modulating several physiological responses, including nociception, anxiety, and depression.[2-4] The two key players involved in EC catabolism are the fatty acid amide hydrolase (FAAH) and the monoacylglycerol lipase (MAGL) enzymes.[5,6] Additionally, the α/β-hydrolase domain containing serine hydrolases, ABHD6 and ABHD12, may act as complementary 2-AG-degrading enzymes in the brain.[7]

FAAH and MAGL are membrane-bound serine hydrolases, which regulate the intracellular levels of AEA, 2-AG and other ECs.[8,9] FAAH utilizes a Ser-Ser-Lys catalytic triad as confirmed by X-ray analysis,[10] and MAGL has a catalytic triad represented by Ser-His-Asp.[11] By elevating the endogenous concentration of their substrates, FAAH and MAGL inhibition can promote beneficial effects on several nervous system disorders, including pain, inflammation, anxiety, and depression[4,12,13] but also on cancer and neuroinflammatory diseases.[14]

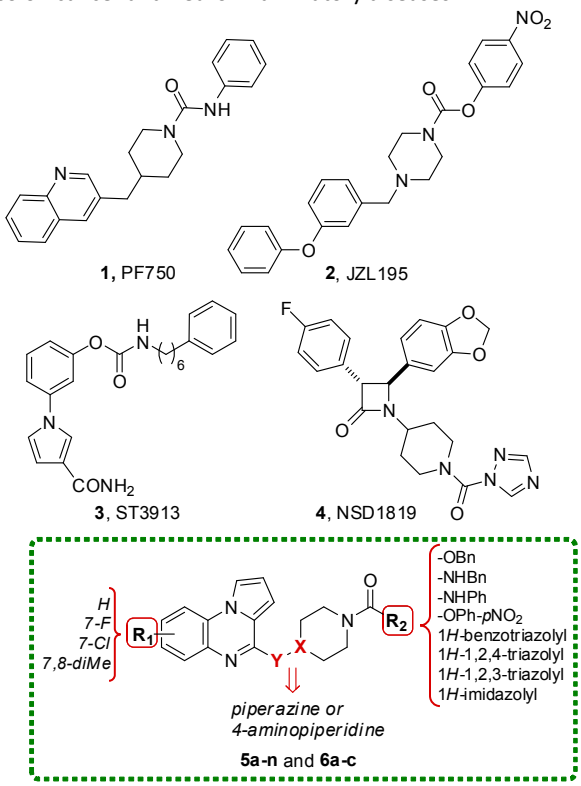

R_1, R_2, X and Y as defined in Table 1

Fig. 1. Reference FAAH, MAGL and dual inhibitors (**1-4**), and title compounds **5a-n** and **6a-c**.

[a] European Research Centre for Drug Discovery and Development (NatSynDrugs), University of Siena, via Aldo Moro 2, 53100 Siena, Italy E-mail: butini3@unisi.it and campiani@unisi.it
[b] Dipartimento di Biotecnologie, Chimica e Farmacia, University of Siena, via Aldo Moro 2, 53100 Siena, Italy
[c] Dipartimento di Farmacia, University of Napoli Federico II, Via D. Montesano 49, 80131, Napoli, Italy
[d] Endocannabinoid Research Group, Institute of Biomolecular Chemistry, C.N.R., Pozzuoli (Napoli), Italy
Electronic Supplementary Information (ESI) available: NMR Spectra and Elemental Analysis Table. See DOI: 10.1039/x0xx00000x

View Article Online
DOI: 10.1039/C6RA12524G

Accordingly, selective inhibition of FAAH and MAGL represents an attractive approach for eliciting the desirable effects of CBR activation with the remarkable benefit of avoiding the classical CBR agonists side effects (hypomotility, hypothermia, catalepsy, and psychotropic effects).[15]

A large number of FAAH inhibitors have been described over the last years, such as α-keto heterocycles, lactams, carbamates, and piperidine-/piperazine-based ureas.[16] To this latter class belong the irreversible piperidine urea compound PF750 (**1**, Fig. 1)[17] and the reversible piperazine urea JNJ-1661010.[18] P750, however, may be classified as a weak FAAH selective inhibitor.

Recently, Cravatt and co-workers described MAGL piperidine carbamate selective inhibitors (e.g. JZL184[19] and KLM-29[20]) and piperazine carbamates dual FAAH/MAGL inhibitors, such as JZL195[21] (**2**, Fig. 1). JZL195 binds both murine brain enzymes in the nanomolar range; however, it is characterized by the hazardous *p*-nitrophenylcarbamate functionality. Recently, Aaltonen and co-workers reported the development of potent piperazine and piperidine urea MAGL inhibitors.[22] In the frame of our research involving endocannabinoid metabolizing enzyme inhibitors, we recently developed phenyl-1-pyrrole-based compounds (typified by compound **3**, Fig. 1) as ultrapotent and selective FAAH reversible inhibitors[23, 24] and the beta-lactam-based piperidintriazole urea **4** (Fig. 1) as an exceptionally potent and selective MAGL inhibitor.[25, 26]

Increasing evidence highlights that a full spectrum of activities is not observed upon inhibition of either FAAH or MAGL enzymes alone,[27-29] therefore exploitation of compounds endowed with a dual inhibition profile could represent a valuable therapeutic approach in pathological states such as neuropathic pain[30] and epilepsy.[31]

Remarkably, the enhancement of both the AEA and 2-AG signalling pathways enables these two ECs to engage in extensive crosstalk.[21] A critical balance between AEA and 2-AG levels, controlled by their synthesizing and metabolizing enzymes, may thus be of pivotal importance for normal physiological processes, as well as to face pathological events.[32-34] Accordingly, systemic administration of the dual FAAH/MAGL inhibitor JZL195 (**2**) reduced allodynia in a chronic constriction injury model of neuropathic pain with greater efficacy with respect to selective FAAH or MAGL inhibitors. Notably, **2** also displayed a better therapeutic window between anti-allodynia and side effects than the CBR agonist WIN55212 and retained anti-allodynia efficacy during repeated treatment.[30]

Furthermore, the dual FAAH/MAGL inhibitor AM6701 resulted more viable against excitotoxic brain injury with respect to the FAAH selective analogue AM6702, showing protection against cytoskeletal damage and synaptic decline in both a brain slice model and *in vivo*, and seizure scores and behavioural deficits were reduced in the kainic acid rat model.[31]

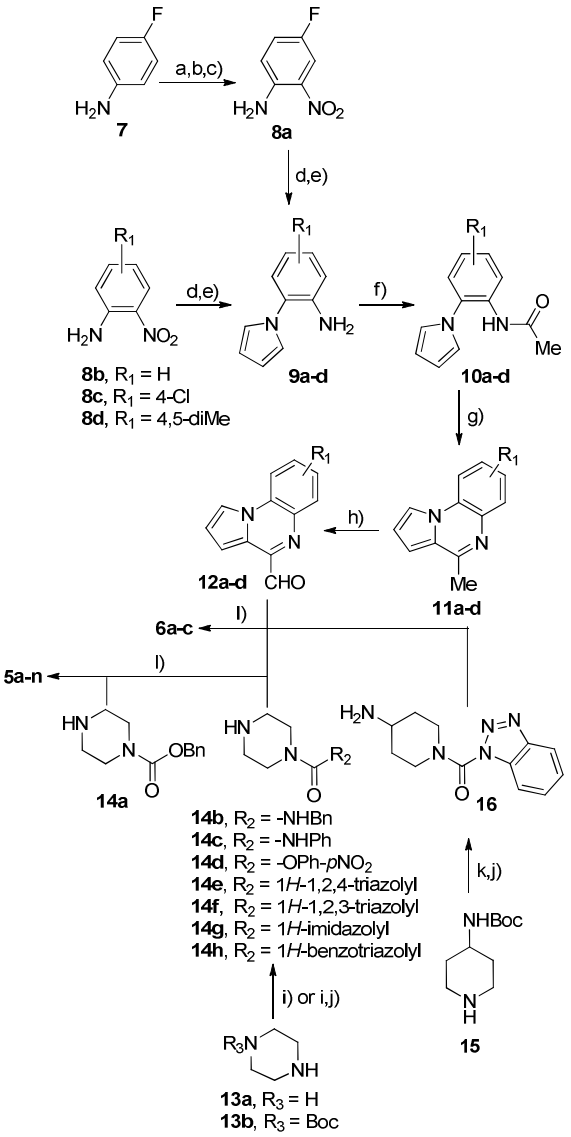

Scheme 1. Synthetic procedures for the preparation of compounds **5a-n** and **6a-c**. Reagents and conditions: (a) Ac_2O, TEA, dry DCM, 0 °C to rt, 1 h; (b) HNO_3, Ac_2O, AcOH, 0 °C to rt, 12 h; (c) 6N HCl, reflux, 4 h; (d) 2,5-dimethoxytetrahydrofuran, 5 N HCl, 1,4-dioxane, 110 °C, 5 min; (e) $SnCl_2{\cdot}H_2O$, EtOAc, reflux, 2 h; (f) AcCl, pyridine, dioxane, reflux, 4 h; (g) $POCl_3$, toluene, reflux, 4 h; (h) SeO_2, 1,4-dioxane, reflux, 4 h; (i) benzyl isocyanate for **14b**, phenyl isocyanate for **14c** or *p*-nitrophenyl chloroformate for **14d**, Et_3N, dry THF, 25 °C, 12 h; 1*H*-1,2,4-triazole for **14e**, 1*H*-1,2,3-triazole for **14f** or 1*H*-benzotriazole for **14h**, phosgene (20 % in toluene), DMAP, dry DCM, 25 °C, 12 h; CDI for **14g**, dry DCM, 25 °C, 12 h; (j) TFA, dry DCM, 25 °C, 2 h; (k) 1*H*-benzotriazole, phosgene (20 % in toluene), DMAP, dry DCM, 25 °C, 12 h; (l) for **5a-c,e**: $NaCNBH_3$, EtOH/AcOH 1%, 25 °C, 12 h; for **5d**, **5f-n**, **6a-c**: $Na(OAc)_3BH$ dry DCM, 25 °C, 12 h.

As a continuation of our efforts in this field, we herein describe the development and structure-activity relationships of a series of novel FAAH and MAGL inhibitors (**5a-n** and **6a-c**, Fig. 1 and Table 1) bearing the pyrroloquinoxaline pharmacogenic system as the key substructure for development of drug-like compounds.[35-42] In the

View Article Online
DOI: 10.1039/C6RA12524G

specific frame of selective or dual acting FAAH/MAGL inhibitors, we envisaged that the appropriate combination and outdistancing between the pyrroloquinoxaline-based scaffold and a piperazine carboxamide/carbamate[43] portion could drive to compounds characterized by suitable size and geometrical shape for fitting both enzymes' binding pockets. To this aim we synthesized compounds **5a-n** (Fig. 1 and Table 1) in which the piperazine carboxamide/carbamate moiety was connected to the C-4 of the pyrroloquinoxaline skeleton by a methylene spacer, perceived as flexibility element for multiple enzyme adaptation. Also compounds **6a-c** (Fig. 1 and Table 1) were synthesised, in which the piperazine moiety was replaced by a 4-aminopiperidine. Inhibition potency of the developed compounds was evaluated on FAAH (from rat brain) and MAGL (from COS cells and rat brain) enzymes. Classical medicinal chemistry approaches coupled with computational analysis and biological evaluation led to the definition of key molecular insights for both selective or dual FAAH/MAGL inhibition. **5e** is the prototype of this new class of inhibitors, which led to **5m**, an analogue with a potency comparable to JZL195 but without the structural drawbacks mentioned above.

Results and discussion

Chemistry

Compounds **5a-n** and **6a-c** were synthesized as described in Scheme 1. The synthesis of the 4-fluoro-2-nitroaniline **8a** was accomplished starting from 4-fluoroaniline (**7**) which was first protected as acetamide and then submitted to a classical nitration protocol. Following acetamide hydrolisis led to the desired aniline.

Aniline **8a** and the commercially available anilines **8b-d** were subjected to Clauson-Kaas reaction and to subsequent reduction of the nitro group with tin(II) chloride, affording the *o*-pyrrolyl anilines **9a-d**.[37] These latter were converted into their corresponding acetamide derivatives **10a-d** and subsequently cyclized in the presence of phosphorus oxychloride to provide the 4-methylpyrroloquinoxaline derivatives **11a-d**.[44] The methyl group was then oxydized to aldehyde by selenium(IV) oxide in 1,4-dioxane.[45] Intermediates **12a-d** underwent reductive amination with the piperazine derivatives **14a-h** or the 4-aminopiperidine **16** leading to final compounds **5a-n** and **6a-c**, respectively.

Structure-activity relationships (SARs)

The inhibition potency of compounds **5a-n** and **6a-c** for FAAH (rat brain membrane) and MAGL (COS cells) enzymes is presented in Table 1; further details are provided in the Experimental Section). Compounds displaying a significant affinity for COS MAGL were further tested against rat brain MAGL (Table 1). Under these conditions, we registered a general ~3-16-fold drop in inhibition potency, with the only exception of **5m**, which was nearly equipotent on both preparations. These data are in line with typical discrepancies previously observed among MAGL inhibitory activities when using enzyme preparations from different animal species. Moreover, compounds **5i**, **5k** and **5m** the most potent inhibitors on MAGL rat brain, were tested on the same enzyme applying a pre-incubation time of 10 and 60 minutes. In agreement with the mechanism of action of "serine trap inhibitors", the tested compounds displayed an increased enzyme inhibitory potency when pre-incubated for 10 min with the enzyme. This pre-incubation time is satisfactory to reach the maximum activity, since the same compounds, when assayed with 60 min pre-incubation, did not show further significant improvement of their inhibitory potency (Table 1).

The analysis of these biological data was performed by means of molecular docking studies which allowed us to better define the key elements for the inhibition of these ECs' catabolizing enzymes.

The first sub-series of compounds, namely **5a-h** (Table 1), feature an unsubstituted pyrroloquinoxaline skeleton bridged at C-4 by a methylene linker to a terminal piperazine carbamate/urea moiety, as the potential electrophilic centre to undergo nucleophilic attack by the target enzymes. In particular, the benzyl carbamate (**5a**) and the benzylurea (**5b**) analogues showed poor inhibition potency on both enzymes being too long to correctly fit within the FAAH and MAGL active sites (not shown). A terminal phenylurea (**5c**) slightly improved potency against FAAH (IC_{50} = 960 nM, Table 1). In fact, docking studies indicated a better positioning within the FAAH catalytic site of **5c**, reaching the central region of the FAAH active site with the phenylurea moiety projected towards F244. Only limited interactions, such as π-π stacking with F192, were observed and no other contacts with the key aromatic residues of the binding site were detected (not shown). Although poorly druggable, but in line with reference FAAH/MAGL inhibitors such as compound **2**, we explored the effect of a *p*-nitrophenylcarbamoyl moiety on our pyrroloquinoxaline-based inhibitors. Derivative **5d** displayed submicromolar inhibition potency for both FAAH and MAGL (FAAH IC_{50} = 562 nM; MAGL IC_{50} = 826 nM, Table 1) enzymes. Introduction of a smaller 1,2,4-triazole urea, a moiety which already demonstrated an optimum potential for MAGL inhibition, robustly improved inhibition.[22] Gratifyingly, compound **5e** showed one of the best inhibitory profile among the synthesized compounds with inhibition potencies in the low nanomolar range against FAAH (IC_{50} = 37 nM, rat brain;) and submicromolar for MAGL (IC_{50} = 44.66 nM, 611.37 nM, COS and rat brain, respectively; Table 1). The output of our docking calculations performed by using Induced Fit Docking (IFD) via Maestro GUI as previously described by us[45-47] (Fig. 2) confirmed the crucial role of the acyltriazole portion for the dual inhibitory activity, coupled to the presence of the methylene linker bridging the pyrroloquinoxaline core and the piperazine moiety. In fact, **5e** revealed a strong pattern of interaction with both target enzymes. The compound spans the gorge of the FAAH enzyme mainly interacting by hydrophobic contacts with the key residues as well as with the catalytic triad (Fig. 2A). The triazole moiety is able to establish a π-π stacking with F192, while the tricyclic portion of **5e** establishes two π-π stacking with F192 and F432. Moreover a series of hydrophobic contacts with I238, L380, F381, L401, L404 M436, and M495 was observed. Additionally, **5e** also H-binds the two catalytic serine residues (S217 and S241) (Fig. 2B). The retrieved binding mode of **5e** in complex with FAAH enzyme is therefore in line with its strong enzyme inhibitory potency. Within

View Article Online
DOI: 10.1039/C6RA12524G

the MAGL binding site, **5e** mainly establishes a series of polar contacts. In fact, the 1,2,4-triazole moiety deeply projects into the enzyme, interacting with the catalytic site by two H-bonds with Y194 and S122 (catalytic serine) and one with the backbone of A51 (oxyanion hole) (Fig. 2C). Furthermore, it establishes a double π-π stacking with the catalytic residue H269 and with H121. The pyrroloquinoxaline system gives a series of hydrophobic contacts with M123, L148, L150, L151, L176, L205, L213, L214, V217 and L241 (Fig. 2D). Notably, the carbonyl group, suitable for undergoing

the nucleophilic attack from the catalytic serine residues, was found at a distance (< 2 Å in both enzymes) appropriate for generating a tetrahedral intermediate in both FAAH and MAGL.

A small set of derivatives was then conceived in order to explore different terminal azole-containing carboxamides, namely compounds **5f**, **5g** and **5h** bearing a 1,2,3-triazole, an imidazole and a benzotriazole ring, respectively. The 1,2,3-triazole-containing compound **5f** led to a considerable drop of affinity for FAAH enzyme (FAAH IC_{50} = 175.50 nM; recombinant MAGL IC_{50} = 39.68 nM, Table 1), while compound **5h** bearing the more hindered benzotriazole moiety led to a dramatic loss of MAGL inhibitory activity (FAAH IC_{50} = 23.59 nM; MAGL IC_{50} = 851.10 nM, Table 1). Therefore, for these two compounds the exploration of different terminal ureas led, to a different extent, to the loss of the dual inhibitory profile, giving molecular insights for selective inhibition. Compound **5g** displayed a loss of affinity for both enzymes.

View Article Online
DOI: 10.1039/C6RA12524G

Table 1. IC_{50} values on FAAH and MAGL enzymes for compounds **5a-n**, **6a-c**, and reference compounds **1** and **4**.

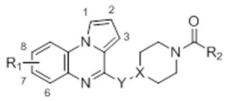

Cpd	X	Y	R_1	R_2	IC_{50} FAAH (nM) [a,b] rat brain membrane	IC_{50} MAGL (nM) [a,b] COS cell cytosol	IC_{50} MAGL (nM) [a] (rat brain cytosol)
5a	N	$-CH_2-$	H		>10,000 [3.73%]	>10,000 [5.08%]	ND[c]
5b	N	$-CH_2-$	H		>10,000 [13.80%]	>10,000 [13.03%]	ND
5c	N	$-CH_2-$	H		960	>10,000 [0%]	ND
5d	N	$-CH_2-$	H	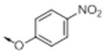	562	826	ND
5e	N	$-CH_2-$	H		37.0	44.7	611
5f	N	$-CH_2-$	H		175	39.7	632
5g	N	$-CH_2-$	H		2210	>10,000	ND
5h	N	$-CH_2-$	H		23.6	851	5000
5i	N	$-CH_2-$	7-F		20.7	49.9	329 4.3[d] 2.1[e]
5j	N	$-CH_2-$	7-F		23.2	388	ND
5k	N	$-CH_2-$	7-Cl		25.1	95.9	284 4.0[d] 3.8[e]
5l	N	$-CH_2-$	7-Cl		35.8	1321	ND
5m	N	$-CH_2-$	7,8-diMe		32.4	80.1	133 4.7[d] 4.2[e]
5n	N	$-CH_2-$	7,8-diMe		27.3	487	ND
6a	-CH-	$-CH_2NH-$	7-F		9.60	1600	ND
6b	-CH-	$-CH_2NH-$	7-Cl		60.4	1950	ND
6c	-CH-	$-CH_2NH-$	7,8-diMe		25.1	1830	ND
1	-	-	-	-	3000	-	-
4					-	-	20.7[d] 6.4[e]

[a]values are means of three experiments (n = 3) and all SD are within 10%; [b]% of enzyme inhibition at the maximum concentration tested is reported in square brackets when IC_{50} is > 10 μM; [c]ND: not determined; [d]assay performed with 10 min of pre-incubation (n = 2); [e]assay performed with 60 min of pre-incubation (n = 3).

View Article Online
DOI: 10.1039/C6RA12524G

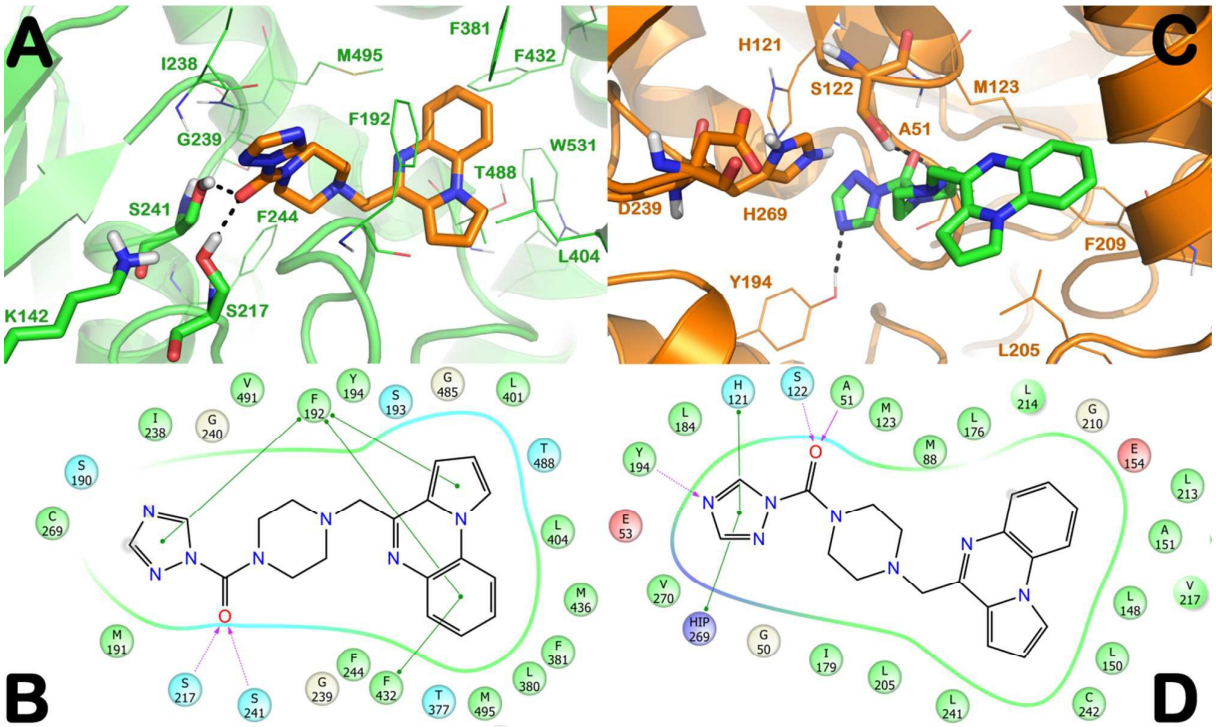

Fig. 2. (A,B) IFD pose and ligand interaction diagram of **5e** (orange sticks) into FAAH enzyme (PDB ID: 3PPM in green cartoon). (C,D) IFD pose and ligand interaction diagram of **5e** (green sticks) into MAGL enzyme (PDB ID: 3HJU in orange cartoon). The catalytic triad of two enzymes is represented by sticks, while the interacting residues are represented by lines. The H-bonds are represented by black dotted lines. The pictures were generated by PyMOL and Maestro (Maestro, version 9.3, Schrödinger, LLC, New York, NY, 2012); HIP stands for protonated histidine.

Our SAR investigation also encompassed the exploration of a small set of structural decorations performed on the pyrroloquinoxaline skeleton. To this aim 7-fluoro-, 7-chloro- and 7,8-dimethyl-substituted derivatives were prepared bearing either a terminal 1,2,4-triazole or a benzotriazole moieties (**5i-n**, Table 1). In general, the 1,2,4-triazole-containing derivatives (**5i**, **5k** and **5m**, Table 1) preserved an excellent dual FAAH/MAGL inhibitory profile, comparable to that displayed by the prototypical dual inhibitor **5e,** with compound **5m** showing the best balance of activities among the enzymes taken under consideration. In line with our previous observations the presence of the benzotriazole carboxamide moiety (**5j**, **5l** and **5n**, Table 1) determined a loss of MAGL affinity.

This trend became even more marked with the last set of derivatives (**6a-c**, Table 1) in which the piperazine benzotriazole carboxamide was replaced by a 4-aminopiperidine benzotriazole carboxamide moiety. Further distancing between the pyrroloquinoxaline portion and the terminal benzotriazole urea led to a dramatic loss of MAGL affinity while preserving an optimum FAAH inhibitory profile. The comparison of docking calculations of compound **5j** with those obtained with compound **5e** provides a clear molecular rationalization for the above observations (Fig. S1 *vs* Fig. 2). Regarding compound **5j** a remarkable activity against FAAH, accompanied by a slight decrease of MAGL affinity was registered. As expected, docking studies suggest for **5j** an accommodation into FAAH (Fig. S1 panels A, B) very similar to that found for **5e** (Fig. 2). On the contrary, the analysis of the docking calculation of **5j** into MAGL (Fig. S1 panels C, D) reveals a slight decrease of contacts into the active site with respect to those found for **5e**. In particular, **5j** does not establish the key interactions with H121 and Y194 (Fig. S1 panels C,D) due to the higher steric hindrance of the benzotriazole moiety.

View Article Online
DOI: 10.1039/C6RA12524G

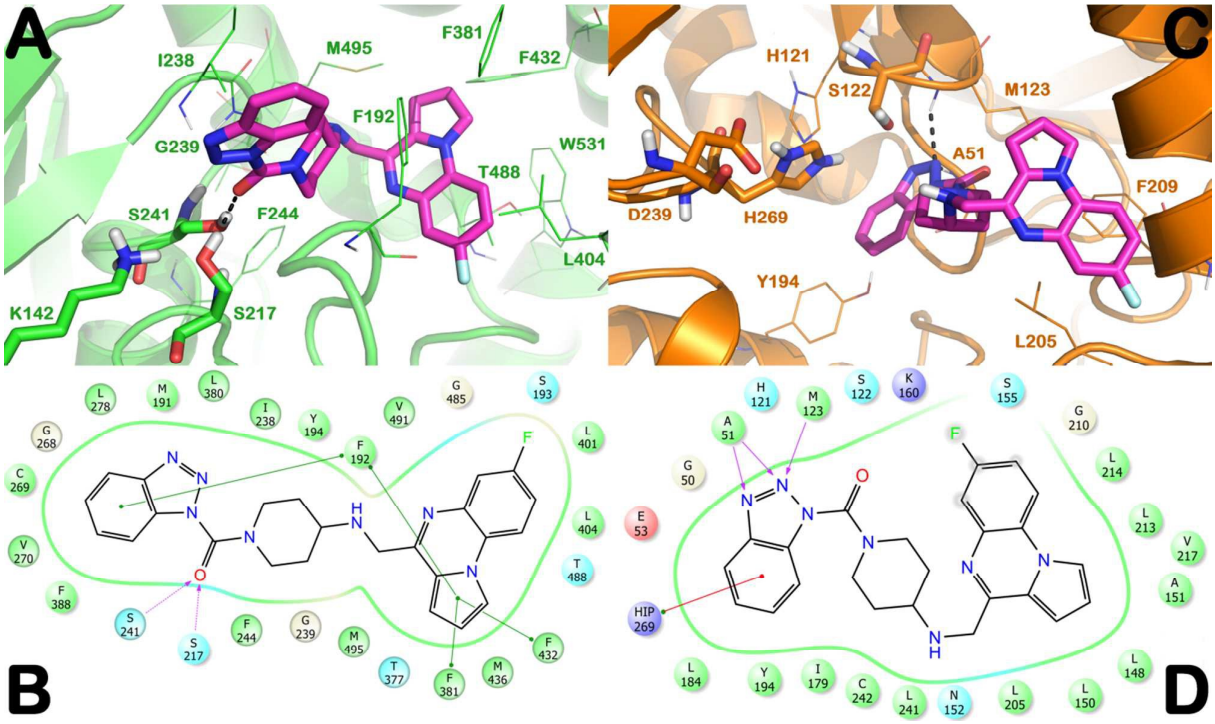

Fig. 3. (A,B) IFD pose and ligand interaction diagram of **6a** (magenta sticks) into FAAH enzyme (PDB ID: 3PPM in green cartoon). (C,D) IFD pose and ligand interaction diagram of **6a** (magenta sticks) into MAGL enzyme (PDB ID: 3HJU in orange cartoon). The catalytic triad of two enzymes is represented by sticks, while the interacting residues are represented by lines. The H-bonds are represented by black dotted lines. The pictures were generated by PyMOL and Maestro (Maestro, version 9.3, Schrödinger, LLC, New York, NY, 2012); HIP stands for protonated histidine.

Regarding compound **6a** (Fig. 3), the computational analysis clearly highlighted the negative effect of the 4-aminopiperidine benzotriazole carboxamide for MAGL inhibition. Based on the activity data reported in Table 1 the structural arrangement of **6a** is well-tolerated by FAAH being this compound one of the best FAAH inhibitors of the series. The output of computational studies reported in Fig. 3A,B for FAAH supports the biological data and clearly evidences the strong pattern of interaction of **6a** within the enzyme. Compound **6a** is potentially able to engage a relevant series of hydrophobic contacts (π-π stacking) with F192, F381 and F432 by its tricyclic portion and the benzotriazole moiety can also establish a π-π stacking with F192 (face-to-edge). Moreover, the carbonyl group is correctly located in front of the catalytic centre establishing H-bonds with the catalytic residues S217 and S241 (Fig. 3A,B). On the contrary, the docking output of **6a** into MAGL (Fig. 3C,D) reveals a limited number of interactions into the active site. The introduction of the 4-aminopiperidine benzotriazole carboxamide portion hampered the compound from completely reaching the MAGL active site. In fact, the acyl-benzotriazole moiety was not able to strongly interact with the catalytic residues and only a cation-π stacking with H269 was observed. Compound **6a** did not interact with the catalytic serine (S122) but only H-bound the backbone of the oxyanion hole residues (A51 and M123), precluding a strong interaction with the enzyme (lacking also some hydrophobic contacts at the boundary of the binding site).

View Article Online
DOI: 10.1039/C6RA12524G

Journal Name

ARTICLE

Next, we evaluated in silico ADME+T properties of five representative compounds (**5d**,**e**,**i**,**j**,**m**, Table S1) by means of QikProp program (QikProp, version 3.5; Schrödinger, LLC: New York, 2012) and TEST software. The output of the calculation indicated satisfactory physico-chemical properties for the title compounds. Moreover, the favorable predicted LD_{50} value coupled to a potential non-mutagenic profile support the drug-like propensity of the developed compounds.

Experimental

Chemistry

Unless otherwise specified, materials were purchased from commercial suppliers and used without further purification. Reaction progress was monitored by TLC using silica gel 60 F254 (0.040-0.063 mm) with detection by UV. Silica gel 60 (0.040-0.063 mm) was used for column chromatography. ^{1}H NMR spectra were recorded on a Varian 300 MHz spectrometer or a Bruker 400 MHz spectrometer by using the residual signal of the deuterated solvent as internal standard. Splitting patterns are described as singlet (s), doublet (δ), triplet (t), quartet (q), and broad (br); the value of chemical shifts (δ) are given in ppm and coupling constants (*J*) in Hertz (Hz). ESI-MS spectra were performed by an Agilent 1100 Series LC/MSD spectrometer. Yields refer to purified products and are not optimized. Elemental analyses (reported in Table S2) were performed in a Perkin Elmer 240C elemental analyser, and the results were within ± 0.4% of the theoretical values.

4-Fluoro-2-nitroaniline (8a). To a stirred solution of 4-fluoronaniline (**7**, 10.0 g, 90.00 mmol) and triethylamine (18.6 mL, 134.00 mmol) in DCM (50 mL), acetic anhydride (9.3 mL, 99.00 mmol) was added dropwise at 0 °C and the resulting mixture was stirred for 1 h at 25 °C. 1 N HCl was added and the aqueous phase was extracted with EtOAc (3 x 50 mL). The combined organic layers were washed with a saturated solution of NaCl, dried over anhydrous Na_2SO_4, filtered and concentrated to give pure *N*-(4-fluorophenyl)acetamide (quantitative yield). ^{1}H NMR (300 MHz, $CDCl_3$) δ 7.70 (s, 1H), 7.45 (t, *J* = 8.8 Hz, 2H), 6.98 (t, *J* = 8.7 Hz, 2H), 2.14 (s, 3H); ESI-MS *m/z* 154 [*M*+H]$^+$. *N-(4-Fluoro-2-nitrophenyl)acetamide*. *N*-(4-Fluorophenyl)acetamide (12.7 g, 83.25 mmol) was dissolved in acetic acid (40 mL), then trifluoroacetic anhydride (40 mL) and concentrated HNO_3 (7.4 mL) were added dropwise at 0 °C. The mixture was stirred for 12 h at 25 °C and a saturated solution of $NaHCO_3$ solution was added. The aqueous phase was extracted with EtOAc (3 x 50 mL) and the combined organic layers were washed with a saturated solution of NaCl, dried over anhydrous Na_2SO_4, filtered and concentrated to afford title compound (quantitative yield) as a yellow solid. ^{1}H NMR (300 MHz, $CDCl_3$) δ 10.13 (br s, 1H), 8.74 (dd, *J* = 9.4, 5.2 Hz, 1H), 7.89 (dd, *J* = 8.5, 2.9 Hz, 1H), 7.41-7.31 (m, 1H), 2.27 (s, 3H); ESI-MS *m/z* 199 [*M*+H]$^+$. A mixture of *N*-(4-fluoro-2-nitrophenyl)acetamide (6.0 g, 38.45 mmol) in 6 N HCl (40 mL) was refluxed for 4 h. After cooling to 25 °C, the mixture was neutralized with aqueous $NaHCO_3$ and extracted with EtOAc (3 x 20 mL). The combined organic layers were washed with a saturated solution of NaCl, dried over anhydrous Na_2SO_4, filtered and concentrated. Silica gel column chromatography (PetEt/Et_2O 5:1) afforded title compound as light yellow solid (70% yield). ^{1}H NMR (300 MHz, $CDCl_3$) δ 7.82 (dd, *J* = 9.1, 3.0 Hz, 1H), 7.17 (dd, *J* = 10.0, 7.2 Hz, 1H), 6.80 (d, *J* = 9.2 Hz, 1H), 5.96 (br s, 2H); ESI-MS *m/z* 157 [*M*+H]$^+$.

5-Fluoro-2-(1*H*-pyrrol-1-yl)aniline (9a). *1-(4-Fluoro-2-nitrophenyl)-1H-pyrrole*. A solution of **8a** (2.5 g, 16.00 mmol) and 2,5-dimethoxytetrahydrofuran (2.1 mL, 16.00 mmol) in 1,4-dioxane (40 mL) was heated to reflux. Then 5 N HCl (4 mL) was added and, after 5 min, the reaction mixture was diluted with cold water until a white precipitate was formed. The aqueous phase was extracted with $CHCl_3$ (3 x 20 mL) and the combined organic layers were dried over anhydrous Na_2SO_4, filtered and concentrated to obtain 1-(4-fluoro-2-nitrophenyl)-1*H*-pyrrole (95% yield) as a pale yellow oil that was used in the following step without further purification; ^{1}H NMR (300 MHz, $CDCl_3$) δ 7.61 (dd, *J* = 7.5, 2.8 Hz, 1H), 7.48 (dd, *J* = 8.8, 5.0 Hz, 1H), 7.42-7.33 (m, 1H), 6.75 (t, *J* = 2.1 Hz, 1H), 6.36 (t, *J* = 2.2 Hz, 2H); ESI-MS *m/z* 207 [*M*+H]$^+$; To a solution of this latter (3.1 g, 15.20 mmol) in EtOAc (75 mL), $SnCl_2{\cdot}2H_2O$ (20.6 g, 91.20 mmol) was added and the solution was refluxed for 2 h. Then the reaction mixture was quenched with saturated aqueous $NaHCO_3$ and filtered through Celite. The aqueous phase was extracted with EtOAc (3 x 25 mL), and the combined organic layers were dried over anhydrous Na_2SO_4, filtered and concentrated. The crude residue was purified by automated flash chromatography using a silica gel pre-packed column (PetEt/Et_2O 15:1) to afford title compound (85% yield) as a colourless oil; ^{1}H NMR (300 MHz, $CDCl_3$) δ 7.14-7.01 (m, 1H), 6.85-6.58 (m, 2H), 6.55-6.41 (m, 2H), 6.34 (t, *J* = 2.0 Hz, 2H), 3.80 (br s, 2H); ESI-MS *m/z* 177 [*M*+H]$^+$.

2-(1*H*-Pyrrol-1-yl)aniline (9b). Starting from **8b** (4.0 g, 28.96 mmol) and 2,5-dimethoxytetrahydrofuran (4.6 mL, 36.20 mmol), *1-(2-nitrophenyl)-1H-pyrrole* was obtained following the same procedure reported for **9a**. ^{1}H NMR (300 MHz, $CDCl_3$) δ 7.85 (dd, *J* = 8.4, 1.4 Hz, 1H), 7.65 (td, *J* = 7.9, 1.5 Hz, 1H), 7.51-7.45 (m, 2H), 6.83-6.76 (m, 2H), 6.40-6.32 (m, 2H); ESI-MS *m/z* 189 [*M*+H]$^+$; Starting from this latter, title compound was prepared according to the procedure

View Article Online
DOI: 10.1039/C6RA12524G

previously described for **9a** (68% yield, over 2 steps); ^{1}H NMR (300 MHz, $CDCl_3$) δ 7.16 (d, *J* = 7.2 Hz, 2H), 6.93-6.76 (m, 4H), 6.40-6.29 (m, 2H), 3.68 (br s, 2H); ESI-MS *m/z* [*M*+H]$^+$ 159 (100).

5-Chloro-2-(1*H*-pyrrol-1-yl)aniline (9c). Starting from **8c** (2.5 g, 14.49 mmol) and 2,5-dimethoxytetrahydrofuran (1.9 mL, 14.49 mmol), *1-(4-chloro-2-nitrophenyl)-1H-pyrrole* was obtained following the same procedure reported for **9a**. ^{1}H NMR (300 MHz, $CDCl_3$) δ 8.32 (d, *J* = 1.4 Hz, 1H), 7.78 (dd, *J* = 7.4, 1.5 Hz, 1H), 7.66 (d, *J* = 7.5 Hz, 1H), 7.21-7.09 (m, 2H), 6.33-6.19 (m, 2H); ESI-MS *m/z* 223 [*M*+H]$^+$. Starting from this latter, title compound was prepared according to the procedure previously described for **9a** (72% yield, over 2 steps). ^{1}H NMR (300 MHz, $CDCl_3$) δ 7.06 (d, *J* = 8.3 Hz, 1H), 6.82-6.77 (m, 2H), 6.77-6.70 (m, 1H), 6.35 (t, *J* = 2.1 Hz, 2H), 3.78 (br s, 2H). ESI-MS *m/z* 193 [*M*+H]$^+$.

4,5-Dimethyl-2-(1*H*-pyrrol-1-yl)aniline (9d). Starting from **8d** (2.5 g, 15.04 mmol) and 2,5-dimethoxytetrahydrofuran (2.0 mL, 15.04 mmol), *1-(4,5-dimethyl-2-nitrophenyl)-1H-pyrrole* was obtained following the same procedure reported for **9a**. ^{1}H NMR (300 MHz, $CDCl_3$) δ 7.68 (s, 1H), 7.22 (s, 1H), 6.81-6.69 (m, 2H), 6.38-6.18 (m, 2H), 2.36 (s, 6H); ESI-MS *m/z* 217 [*M*+H]$^+$. Starting from this latter, title compound was prepared according to the procedure previously described for **9a** (76% yield, over 2 steps); ^{1}H NMR (300 MHz, $CDCl_3$) δ 6.94 (s, 1H), 6.82 (t, *J* = 2.1 Hz, 2H), 6.63 (s, 1H), 6.33 (t, *J* = 2.1 Hz, 2H), 3.53 (br s, 2H), 2.23 (s, 3H), 2.18 (s, 3H); ESI-MS *m/z* 187 [*M*+H]$^+$.

***N*-(5-Fluoro-2-(1*H*-pyrrol-1-yl)phenyl)acetamide (10a).** To a solution of **9a** (110 mg, 0.63 mmol) in 1,4-dioxane (2 mL), pyridine (56 µL, 0.69 mmol) and acetyl chloride (45 µL, 0.63 mmol) were added. The solution was refluxed for 4 h then the solvent was removed. The residue was taken up with water and extracted with EtOAc (3 x 10 mL). The combined organic phases were dried over anhydrous Na_2SO_4, filtered and concentrated. The crude residue was purified by silica gel column chromatography (PetEt/ EtOAc 1:1) to provide title compound (68% yield) as a white amorphous solid; ^{1}H NMR (300 MHz, $CDCl_3$) δ 8.25 (dd, *J* = 10.8, 2.4 Hz, 1H), 7.28-7.18 (m, 1H), 6.96 (br s, 1H), 6.89-6.79 (m, 1H), 6.75 (t, *J* = 2.1 Hz, 2H), 6.40 (t, *J* = 2.1 Hz, 2H), 2.03 (s, 3H); ESI-MS *m/z* 219 [*M*+H]$^+$.

***N*-(2-(1*H*-Pyrrol-1-yl)phenyl)acetamide (10b).** Starting from **9b** (100 mg, 0.63 mmol), the title compound was obtained following the same procedure reported for **10a** (63% yield), after purification by silica gel column chromatography (PetEt/ EtOAc 1:1); ^{1}H NMR (400 MHz, $CDCl_3$) δ 7.78 (d, *J* = 7.8 Hz, 1H), 7.29-7.33 (m, 1H), 7.20 (d, *J* = 7.0 Hz, 1H), 7.07-7.11 (m, 1H), 6.95 (br s, 1H), 6.72 (s, 2H), 6.33 (s, 2H), 1.97 (s, 1H); ESI-MS *m/z* [*M*+H]$^+$ 201 (100), [*M*+Na]$^+$ 223.

***N*-(5-Chloro-2-(1*H*-pyrrol-1-yl)phenyl)acetamide (10c).** Starting from **9c** (100 mg, 0.52 mmol), the title compound was prepared according to the procedure previously described for **10a** (70% yield), after purification by silica gel column chromatography (PetEt/ Et_2O 10:1); ^{1}H NMR (300 MHz, $CDCl_3$) δ 7.60 (d, *J* = 1.4 Hz, 1H), 7.53 (d, *J* = 7.5 Hz, 1H), 7.30 (dd, *J* = 7.4, 1.5 Hz, 1H), 7.25 (br s, 1H), 7.13-7.06 (m, 2H), 6.28-6.21 (m, 2H), 2.24 (s, 3H); ESI-MS *m/z* 219 [*M*+H]$^+$.

***N*-(4,5-Dimethyl-2-(1*H*-pyrrol-1-yl)phenyl)acetamide (10d).** Starting from **9d** (100 mg, 0.54 mmol), the title compound was obtained following the same procedure reported for **10a** (65% yield), after purification by silica gel column chromatography (PetEt/ Et_2O 10:1); ^{1}H NMR (300 MHz, $CDCl_3$) δ 7.47 (s, 1H), 7.40 (s, 1H), 7.25 (br s, 1H), 7.14-7.02 (m, 2H), 6.29-6.17 (m, 2H), 2.38 (s, 6H), 2.24 (s, 3H); ESI-MS *m/z* 229 [*M*+H]$^+$.

7-Fluoro-4-methylpyrrolo[1,2-*a*]quinoxaline (11a). To a solution of **10a** (50 mg, 0.25 mmol) in toluene (2 mL) phosphorous oxychloride (115 µL, 1.25 mmol) was added dropwise and the reaction mixture was refluxed for 4 h. The yellow precipitate was filtered and the resulting solution was washed with saturated aqueous $NaHCO_3$, dried over anhydrous Na_2SO_4, filtered and concentrated to obtain pure title compound (55% yield) as a yellow amorphous solid; ^{1}H NMR (300 MHz, $CDCl_3$) δ 7.88-7.84 (m, 1H), 7.76 (dd, *J* = 9.0, 5.1 Hz, 1H), 7.57 (dd, *J* = 9.6, 2.8 Hz, 1H), 7.29-7.14 (m, 1H), 6.90 (dd, *J* = 4.0, 1.2 Hz, 1H), 6.84 (dd, *J* = 3.9, 2.7 Hz, 1H), 2.71 (s, 3H); ESI-MS *m/z* 201 [*M*+H]$^+$.

4-Methylpyrrolo[1,2-*a*]quinoxaline (11b). Starting from **10b** (47 mg, 0.23 mmol), the title compound was obtained following the same procedure reported for **11a** (59% yield); ^{1}H NMR (300 MHz, $CDCl_3$) δ 8.02-7.90 (m, 2H), 7.84 (d, *J* = 8.1 Hz, 1H), 7.55-7.36 (m, 2H), 6.95 (d, *J* = 2.9 Hz, 1H), 6.89 (d, *J* = 2.6 Hz, 1H), 2.78 (s, 3H); ESI-MS *m/z* 183 [*M*+H]$^+$.

7-Chloro-4-methylpyrrolo[1,2-*a*]quinoxaline (11c). Starting from **10c** (50 mg, 0.21 mmol), the title compound was obtained following the same procedure reported for **11a** (52% yield); ^{1}H NMR (300 MHz, $CDCl_3$) δ 7.88 (dd, *J* = 7.0, 1.9 Hz, 2H), 7.75 (d, *J* = 8.7 Hz, 1H), 7.43 (dd, *J* = 8.7, 2.3 Hz, 1H), 6.87 (dt, *J* = 32.2, 14.7 Hz, 2H), 2.72 (s, 3H); ESI-MS *m/z* 217 [*M*+H]$^+$.

4,7,8-Trimethylpyrrolo[1,2-*a*]quinoxaline (11d). Starting from **10d** (50 mg, 0.22 mmol), the title compound was obtained following the same procedure reported for **11a** (50% yield); ^{1}H NMR (300 MHz, $CDCl_3$) δ 7.84 (s, 1H), 7.66 (s, 1H), 7.59 (s, 1H), 6.83 (dt, *J* = 6.5, 2.4 Hz, 2H), 2.70 (s, 3H), 2.43 (s, 3H), 2.39 (s, 3H); ESI-MS *m/z* 211 [*M*+H]$^+$.

7-Fluoropyrrolo[1,2-*a*]quinoxaline-4-carbaldehyde (12a). To a solution of **11a** (100 mg, 0.50 mmol) in 1,4-dioxane (2 mL), selenium dioxide (83 mg, 0.75 mmol) was added. The resulting suspension was refluxed for 4 h and then cooled to 25 °C, filtered and dried by rotary evaporation. The residue was purified by silica gel column chromatography (PetEt/EtOAc 5:1) to obtain title compound (56% yield) as a yellowish solid;); ^{1}H NMR (300 MHz, $CDCl_3$) δ 10.10 (s, 1H), 8.01 (s, 1H), 7.93-7.88 (m, 1H), 7.80 (d, *J* = 9, 1H), 7.7-7.68 (m, 1H), 7.46-7.39 (m, 1H), 7.04-7.01 (m, 1H); ESI-MS *m/z* 215 [*M*+H]$^+$.

Pyrrolo[1,2-*a*]quinoxaline-4-carbaldehyde (12b). Starting from **11b** (100 mg, 0.55 mmol), the title compound was obtained following the same procedure reported for **12a** (53% yield), after purification by silica gel column chromatography (PetEt/EtOAc 5:1); ^{1}H NMR (300 MHz, $CDCl_3$) δ 10.13 (s, 1H), 8.13 (d, *J* = 8.1 Hz, 1H), 8.04 (d, *J* = 1.5 Hz, 1H), 7.94 (d, *J* = 8.3 Hz, 1H), 7.74-7.61 (m, 2H), 7.54 (t, *J* = 7.7 Hz, 1H), 7.06-6.98 (m, 1H).

7-Chloropyrrolo[1,2-*a*]quinoxaline-4-carbaldehyde (12c). Starting from **11c** (100 mg, 0.46 mmol), the title compound was obtained following the same procedure reported for **12a** (50% yield) after purification by silica gel column chromatography (PetEt/EtOAc 5:1);

View Article Online
DOI: 10.1039/C6RA12524G

^{1}H NMR (300 MHz, $CDCl_3$) δ 10.09 (s, 1H), 8.12 (d, *J* = 2.2 Hz, 1H), 8.01 (s, 1H), 7.87 (d, *J* = 8.9 Hz, 1H), 7.72-7.57 (m, 2H), 7.07-6.98 (m, 1H); ESI-MS *m/z* 231 [*M*+H]$^+$.

7,8-Dimethylpyrrolo[1,2-*a*]quinoxaline-4-carbaldehyde (12d). Starting from **11d** (100 mg, 0.48 mmol), the title compound was obtained following the same procedure reported for **12a** (40% yield) after purification by silica gel column chromatography (PetEt/EtOAc 5:1); ^{1}H NMR (300 MHz, $CDCl_3$) δ 10.09 (s, 1H), 7.95 (s, 1H), 7.87 (s, 1H), 7.68-7.63 (m, 2H), 6.99-6.95 (m, 1H), 2.50 (s, 3H), 2.43 (s, 3H); ESI-MS *m/z* 225 [*M*+H]$^+$.

***N*-Benzylpiperazine-1-carboxamide (14b).** To a solution of piperazine (**13a**, 100 mg, 1.16 mmol) in dry THF (5 mL), benzyl isocyanate (154 mg, 1.16 mmol) and triethylamine (645 µL, 4.04 mmol) were sequentially added dropwise. The reaction mixture was stirred at 25 °C for 12 h, then volatiles were removed by rotary evaporation. Silica gel column chromatography (DCM/MeOH 5:1) afforded title compound (53% yield) as a colourless oil; ^{1}H NMR (300 MHz, CD_3OD) δ 7.40-7.11 (m, 5H), 4.35 (s, 2H), 3.80-3.56 (m, 4H), 3.25-3.09 (m, 4H).

***N*-Phenylpiperazine-1-carboxamide (14c).** Starting from piperazine (**13a**, 100 mg, 1.16 mmol), phenyl isocyanate (127 µL, 1.16 mmol) and triethylamine (645 µL, 4.04 mmol), the title compound was prepared according to the procedure previously described for **14b**. The residue was purified by silica gel column chromatography (DCM/MeOH 5:1) to obtain pure compound (65% yield) as a white amorphous solid; ^{1}H NMR (300 MHz, CD_3OD) δ 7.45-7.33 (m, 2H), 7.27 (t, *J* = 7.7 Hz, 2H), 7.03 (t, *J* = 7.4 Hz, 1H), 3.84-3.73 (m, 4H), 3.29-3.22 (m, 4H).

4-Nitrophenyl piperazine-1-carboxylate (14d). Starting from piperazine (**13a**, 130 mg, 1.50 mmol), 4-nitrophenylchloroformate (272 mg, 1.35 mmol) and triethylamine (630 µL, 4.50 mmol), title compound was prepared according to the procedure previously described for **14b**. Silica gel column chromatography (DCM/MeOH 10:1) afforded pure compound (45% yield) as a yellow amorphous solid; ^{1}H NMR (300 MHz, $CDCl_3$) δ 8.25 (d, *J* = 9.0 Hz, 2H), 7.30 (d, *J* = 9.0 Hz, 2H), 3.73-3.51 (m, 4H), 3.01-2.89 (m, 4H).

Piperazin-1-yl(1*H*-1,2,4-triazol-1-yl)methanone (14e). *tert-Butyl-4-(1H-1,2,4-triazole-1-carbonyl)piperazine-1-carboxylate*. 1*H*-1,2,4-triazole (100 mg, 1.45 mmol), phosgene (20% solution in toluene, 715 µL, 1.45 mmol) and dimethylaminopiridine (354 mg, 2.90 mmol) were sequentially dissolved in dry DCM (5 mL) and stirred at 25 °C for 30 min. Then 4-Boc-piperazine (**13b**, 135 mg, 0.73 mmol) was added and the reaction mixture was stirred at 25 °C for 12 h. Volatiles were then removed by rotary evaporation. Silica gel column chromatography (DCM/MeOH 20:1) afforded *tert*-butyl-4-(1*H*-1,2,4-triazole-1-carbonyl)piperazine-1-carboxylate (42% yield) as a pale yellow oil. ^{1}H NMR (300 MHz, $CDCl_3$) δ 8.74 (s, 1H), 7.93 (s, 1H), 3.85-3.65 (m, 4H), 3.49 (m, 4H), 1.40 (s, 9H). ESI-MS *m/z* [*M*+H]$^+$ 282. This latter was then dissolved in dry DCM and trifluoroacetic acid (700 µL) was added. The reaction mixture was stirred at 25 °C for 2 h. Solvents were removed by rotary evaporation and the residue was dissolved in EtOAc, treated with a saturated solution of $NaHCO_3$, dried over anhydrous Na_2SO_4, filtered and concentrated. Title compound was obtained in quantitative yield and carried on without further purification; ^{1}H NMR (300 MHz, CD_3OD) δ 9.02 (s, 1H), 8.15 (s, 1H), 4.22-3.98 (m, 4H), 3.45-3.34 (m, 4H). ESI-MS *m/z* [*M*+H]$^+$ 182.

Piperazin-1-yl(1*H*-1,2,3-triazol-1-yl)methanone (14f). Starting from 1*H*-1,2,3-triazole (100 mg, 1,45 mmol), phosgene (20% solution in toluene, 715 µL, 1.45 mmol) and DMAP (354 mg, 2.90 mmol), *tert*-butyl 4-(1*H*-1,2,3-triazole-1-carbonyl)piperazine-1-carboxylate was obtained following the same procedure reported for **14e** (50% yield), after purification by silica gel column chromatography (DCM/MeOH 20:1). ^{1}H NMR (300MHz, $CDCl_3$) δ 8.98 (d, *J* = 7.5 Hz, 1H), 8.38 (d, *J* = 7.5 Hz, 1H), 3.84-3.67 (m, 4H), 3.51-3.29 (m, 4H), 1.50 (s, 9H); ESI-MS *m/z* 282 [*M*+H]$^+$. Starting from this latter, title compound was prepared according to the procedure previously described for **14e** (quantitative yield); ^{1}H NMR (300 MHz, CD_3OD) δ 8.02 (s, 2H), 4.15-4.00 (m, 4H), 3.50-3.37 (m, 4H); ESI-MS *m/z* 182 [*M*+H]$^+$.

(1*H*-Imidazol-1-yl)(piperazin-1-yl)methanone (14g). *tert-butyl-4-(1H-imidazole-1-carbonyl)piperazine-1-carboxylate*. To a solution of 4-Boc-piperazine (**13b**, 100 mg, 0.54 mmol) in dry DCM (10 mL), 1,1-carbonyldiimidazole (96 mg, 0.59 mmol) was added and the reaction was stirred at 25 °C for 12 h. Volatiles were removed under reduced pressure. The crude was purified by silica gel column chromatography (PetEt/EtOAc 1:1) to afford intermediate *tert*-butyl 4-(1*H*-imidazole-1-carbonyl)piperazine-1-carboxylate (51% yield) as a transparent oil. ^{1}H NMR (300 MHz, $CDCl_3$) δ 7.98 (d, *J* = 7.5 Hz, 1H), 7.82 (s, 1H), 7.07 (d, *J* = 7.5 Hz, 1H), 3.69 (dt, *J* = 20.2, 5.1 Hz, 4H), 3.37 (dt, *J* = 15.4, 5.0 Hz, 4H), 1.50 (s, 9H); ESI-MS *m/z* 281 [*M*+H]$^+$. Starting from this latter, title compound was prepared according to the procedure previously described for **14e** (quantitative yield). ^{1}H NMR (300 MHz, CD_3OD) δ 9.38 (s, 1H), 7.95 (s, 1H), 7.69 (s, 1H), 3.98-3.81 (m, 4H), 3.51-3.35 (m, 4H); ESI-MS *m/z* 181 [*M*+H]$^+$.

(1*H*-Benzo[*d*][1,2,3]triazol-1-yl)(piperazin-1-yl)methanone (14h). Starting from 1*H*-benzotriazole (100 mg, 0.84 mmol), phosgene (20% solution in toluene, 415 µL, 0.84 mmol) and DMAP (205 mg, 2.90 mmol), *tert*-butyl 4-(1*H*-benzo[*d*][1,2,3]triazole-1-carbonyl)piperazine-1-carboxylate was obtained following the same procedure reported for **14e** (56% yield), after purification by silica gel column chromatography (PetEt/EtOAc 2:1). ^{1}H NMR (300 MHz, $CDCl_3$) δ 7.96 (d, *J* = 8.2 Hz, 1H), 7.87 (d, *J* = 8.3 Hz, 1H), 7.48 (t, *J* = 7.7 Hz, 1H), 7.30 (t, *J* = 7.6 Hz, 1H), 3.79 (m, 4H), 3.65-3.41 (m, 4H), 1.39 (s, 9H); ESI-MS *m/z* 332 [*M*+H]$^+$. Starting from this latter, title compound was prepared according to the procedure previously described for **14e** (quantitative yield). ^{1}H NMR (300 MHz, CD_3OD) δ 8.10 (d, *J* = 8.3 Hz, 1H), 8.02 (d, *J* = 8.3 Hz, 1H), 7.69 (t, *J* = 7.7 Hz, 1H), 7.54 (t, *J* = 7.7 Hz, 1H), 4.32-4.05 (m, 4H), 3.61-3.41 (m, 4H); ESI-MS *m/z* 232 [*M*+H]$^+$.

(4-Aminopiperidin-1-yl)(1*H*-benzo[*d*][1,2,3]triazol-1-yl)methanone (16). Starting from 4-(Boc-amino)piperidine (**15**, 100 mg, 0.50 mmol) and 1*H*-benzotriazole (120 mg, 1.00 mmol), *tert*-butyl-(1-(1*H*-benzo[*d*][1,2,3]triazole-1-carbonyl)piperidin-4-yl)carbamate was obtained following the same procedure reported for **14e** (56% yield), after purification by silica gel column chromatography (PetEt/EtOAc 2:1). ^{1}H NMR (300 MHz, $CDCl_3$) δ 8.09 (d, *J* = 8.3 Hz,

View Article Online
DOI: 10.1039/C6RA12524G

1H), 7.96 (d, *J* = 8.3 Hz, 1H), 7.60 (t, *J* = 7.7 Hz, 1H), 7.45 (t, *J* = 7.7 Hz, 1H), 4.71-4.36 (m, 3H), 3.93-3.65 (m, 1H), 3.29 (t, *J* = 12.0 Hz, 2H), 2.13 (d, *J* = 11.5 Hz, 2H), 1.63 (q, *J* = 15.3 Hz, 2H), 1.45 (s, 9H); ESI-MS *m/z* 346 [*M*+H]$^+$. Starting from this latter, title compound was prepared according to the procedure previously described for **14e** (quantitative yield). ^{1}H NMR (300 MHz, CD_3OD) δ 8.10 (d, *J* = 8.3 Hz, 1H), 7.96 (d, *J* = 8.3 Hz, 1H), 7.68 (t, *J* = 7.7 Hz, 1H), 7.53 (t, *J* = 7.7 Hz, 1H), 4.68-4.46 (m, 2H), 3.66-3.45 (m, 1H), 3.43-3.30 (m, 2H), 2.29-2.10 (m, 2H), 1.83 (qd, *J* = 12.4, 4.5 Hz, 2H); ESI-MS *m/z* 246 [*M*+H]$^+$.

Benzyl-4-(pyrrolo[1,2-*a*]quinoxalin-4-ylmethyl)piperazine-1-carboxylate (5a). Compound **12b** (57 mg, 0.29 mmol) was dissolved in a 99:1 ethanol/acetic acid mixture (3 mL), then commercially available benzyl piperazine-1-carboxylate (**14a**, 64 mg, 0.29 mmol) was added and the resulting solution was stirred at 25 °C for 1 h. $NaCNBH_3$ was added and the mixture was stirred at 25 °C for 12 h. A saturated solution of $NaHCO_3$ was added and ethanol was removed by rotary evaporation. The aqueous phase was extracted with $CHCl_3$ (3 x 10 mL) and the combined organic layers were dried over anhydrous Na_2SO_4, filtered and concentrated. The crude residue was purified by silica gel column chromatography ($CHCl_3$/MeOH 100:1) to obtain title compound (57% yield) as a white amorphous solid. ^{1}H NMR (400 MHz, $CDCl_3$) δ 7.96 (d, *J* = 8.0 Hz, 1H), 7.93- 7.89 (m, 1H), 7.83 (d, *J* = 8.1 Hz, 1H), 7.50 (t, *J* = 7.7 Hz, 1H), 7.42 (t, *J* = 7.6 Hz, 1H), 7.38-7.26 (m, 5H), 7.15 (d, *J* = 3.9 Hz, 1H), 6.87-6.83 (m, 1H), 5.11 (s, 2H), 3.93 (s, 2H), 3.64-3.47 (m, 4H), 2.77-2.50 (m, 4H); ^{13}C NMR (100 MHz, $CDCl_3$) δ 155.5, 153.1, 137.0, 135.7. 130.2, 128.7, 128.2, 128.1, 127.8, 127.7, 126.1, 125.3, 114.4, 113.9, 113.8, 107.5, 67.3, 53.4, 53.1, 44.0. ESI-MS *m/z* [*M*+H]$^+$ 401 (100), [*M*+Na]$^+$ 423.

***N*-Benzyl-4-(pyrrolo[1,2-*a*]quinoxalin-4-ylmethyl)piperazine-1-carboxamide (5b).** Starting from **12b** (18 mg, 0.09 mmol) and **14b** (20 mg, 0.09 mmol), title compound was prepared according to the procedure previously described for **5a**. Silica gel column chromatography ($CHCl_3$/MeOH 100:1) gave pure compound (71% yield) as a colourless oil. ^{1}H NMR (400 MHz, $CDCl_3$) δ 7.95 (dd, *J* = 7.9, 1.1 Hz, 1H), 7.90 (d, *J* = 1.4 Hz, 1H), 7.82 (d, *J* = 8.0 Hz, 1H), 7.52-7.45 (m, 1H), 7.45-7.38 (m, 1H), 7.33-7.19 (m, 5H), 7.14 (dd, *J* = 3.8, 0.8 Hz, 1H), 6.84 (t, *J* = 3.7 Hz, 1H), 4.76 (t, *J* = 5.1 Hz, 1H), 4.40 (d, *J* = 5.4 Hz, 2H), 3.88 (s, 2H), 3.46-3.37 (m, 4H), 2.70-2.55 (m, 4H); ^{13}C NMR (75 MHz, $CDCl_3$) δ 157.89, 153.1, 139.7, 135.7, 130.2, 128.8, 128.0, 127.8, 127.7, 127.5, 126.0, 125.3, 114.4, 113.9, 113.8, 107.6, 63.1, 53.4, 45.2, 44.0; ESI-MS *m/z* [*M*+H]$^+$ 400.

***N*-Phenyl-4-(pyrrolo[1,2-*a*]quinoxalin-4-ylmethyl)piperazine-1-carboxamide (5c).** Starting from **12b** (51 mg, 0.26 mmol) and **14c** (53 mg, 0.26 mmol), title compound was prepared according to the procedure previously described for **5a**. Silica gel column chromatography ($CHCl_3$/MeOH 100:1) provided pure compound (83% yield) as a white amorphous solid. ^{1}H NMR (300 MHz, $CDCl_3$) δ 7.97 (dd, *J* = 7.9, 1.5 Hz, 1H), 7.94-7.89 (m, 1H), 7.83 (dd, *J* = 8.1, 1.3 Hz, 1H), 7.55-7.38 (m, 2H), 7.38-7.29 (m, 2H), 7.29-7.18 (m, 2H), 7.15 (dd, *J* = 4.0, 1.3 Hz, 1H), 7.04-6.93 (m, 1H), 6.86 (dd, *J* = 4.0, 2.7 Hz, 1H), 6.61 (br s, 1H), 3.89 (s, 2H), 3.56-3.46 (m, 4H), 2.67-2.57 (m, 4H); ^{13}C NMR (75 MHz, $CDCl_3$) δ 155.3, 153.1, 139.2, 135.7, 130.2, 129.1, 127.9, 127.7, 126.0, 125.4, 123.3, 120.2, 114.4, 113.9, 113.8, 107.5, 63.0, 53.4, 44.3; ESI-MS *m/z* [*M*+H]$^+$ 386.

4-Nitrophenyl-4-(pyrrolo[1,2-*a*]quinoxalin-4-ylmethyl)piperazine-1-carboxylate (5d). Starting from **12b** (15 mg, 0.08 mmol) and **14d** (20 mg, 0.08 mmol), title compound was prepared according to the procedure previously described for **5a**. Column chromatography on Al_2O_3 (*n*-Hex/EtOAc 3:1) afforded pure compound (55% yield) as a pale yellow oil. ^{1}H NMR (300 MHz, $CDCl_3$) δ 8.24 (d, *J* = 9.2 Hz, 2H), 8.01 (d, *J* = 7.6 Hz, 1H), 7.98-7.94 (m, 1H), 7.88 (dd, *J* = 8.1, 1.3 Hz, 1H), 7.59-7.42 (m, 2H), 7.29 (d, *J* = 9.2 Hz, 2H), 7.19 (d, *J* = 3.0 Hz, 1H), 6.94-6.87 (m, 1H), 4.01 (s, 2H), 3.83-3.56 (m, 4H), 2.90-2.61 (m, 4H); ESI-MS *m/z* [*M*+H]$^+$ 432 (100), [*M*+Na]$^+$ 454.

(4-(Pyrrolo[1,2-*a*]quinoxalin-4-ylmethyl)piperazin-1-yl)(1*H*-1,2,4-triazol-1-yl)methanone (5e). Starting from **12b** (15 mg, 0.08 mmol) and **14e** (14 mg, 0.08 mmol), title compound was prepared according to the procedure previously described for **5a**. Silica gel column chromatography ($CHCl_3$/MeOH 100:1 to 70:1) provided pure compound (57% yield) as a pale yellow solid. ^{1}H NMR (300 MHz, $CDCl_3$) δ 8.78 (s, 1H), 8.03-7.92 (m, 3H), 7.86 (dd, *J* = 8.1, 1.4 Hz, 1H), 7.57-7.39 (m, 2H), 7.15 (dd, *J* = 4.0, 1.2 Hz, 1H), 6.88 (dd, *J* = 4.0, 2.7 Hz, 1H), 4.08-3.76 (m, 6H), 2.88-2.70 (m, 4H); ^{13}C NMR (75 MHz, $CDCl_3$) δ 152.6, 152.2, 148.7, 146.9, 135.7, 130.2, 128.0, 127.7, 126.0, 125.5, 114.6, 114.0, 113.9, 107.4, 62.5, 53.6, 53.4; ESI-MS *m/z* [*M*+H]$^+$ 362 (100), [*M*+Na]$^+$ 384.

(4-(Pyrrolo[1,2-*a*]quinoxalin-4-ylmethyl)piperazin-1-yl)(1*H*-1,2,3-triazol-1-yl)methanone (5f). Starting from **12b** (15 mg, 0.08 mmol) and **14f** (14 mg, 0.08 mmol), title compound was prepared according to the procedure previously described for **5a**. Silica gel column chromatography (EtOAc) provided pure compound (30% yield) as a pale yellow solid; ^{1}H NMR (300 MHz, $CDCl_3$) δ 8.16 (d, *J* = 1.2 Hz, 1H), 8.02-7.92 (m, 2H), 7.86 (d, *J* = 8.2 Hz, 1H), 7.71 (d, *J* = 1.2 Hz, 1H), 7.55-7.42 (m, 2H), 7.15 (d, *J* = 3.9 Hz, 1H), 6.92-6.84 (m, 1H), 3.99 (s, 2H), 3.88 (m, 4H), 2.81 (m, 4H); ^{13}C NMR (75 MHz, $CDCl_3$) δ 152.6, 148,7, 136.2, 133.1, 130.2, 127.9, 127.7, 126.0, 125.6, 125.4, 114.6, 113.9, 113.8, 107.4, 62.35, 53.1, 52.9; ESI-MS *m/z* 362 [*M*+H]$^+$.

(1*H*-Imidazol-1-yl)(4-(pyrrolo[1,2-*a*]quinoxalin-4-ylmethyl)piperazin-1-yl)methanone (5g). Starting from **12b** (15 mg, 0.08 mmol) and **14g** (14 mg, 0.08 mmol), title compound was prepared according to the procedure previously described for **5a**. Silica gel column chromatography (EtOAc) provided pure compound (35% yield) as a colourless oil; ^{1}H NMR (300 MHz, $CDCl_3$) δ 8.01-7.92 (m, 2H), 7.90-7.82 (m, 2H), 7.57-7.40 (m, 2H), 7.21-7.15 (m, 1H), 7.12 (dd, *J* = 4.0, 1.2 Hz, 1H), 7.10-7.06 (m, 1H), 6.88 (dd, *J* = 3.9, 2.8 Hz, 1H), 3.96 (s, 2H), 3.73-3.60 (m, 4H), 2.81-2.66 (m, 4H); ^{13}C NMR (75 MHz, $CDCl_3$) δ 152.4, 150.9, 137.1, 135.7, 130.2, 129.9, 128.0, 127.7, 125.9, 125.5, 118.1, 114.6, 114.0, 113.9, 107.3, 62.7, 53.3, 46.7; ESI-MS *m/z* 361 [*M*+H]$^+$.

(1*H*-Benzo[*d*][1,2,3]triazol-1-yl)(4-(pyrrolo[1,2-*a*]quinoxalin-4-ylmethyl)piperazin-1-yl)methanone (5h). Starting from **12b** (15 mg, 0.08 mmol) and **14h** (19 mg, 0.08 mmol), title compound was prepared according to the procedure previously described for **5a**. Silica gel column chromatography (PetEt/EtOAc 2:1) provided pure compound (32% yield) as a colourless oil; ^{1}H NMR (300 MHz, $CDCl_3$)

View Article Online
DOI: 10.1039/C6RA12524G

δ 8.08 (d, *J* = 8.3 Hz, 1H), 8.04-7.93 (m, 3H), 7.87 (d, *J* = 8.1 Hz, 1H), 7.64-7.38 (m, 4H), 7.18 (d, *J* = 3.9 Hz, 1H), 6.91-6.80 (m, 1H), 4.00 (m, 6H), 2.85 (m, 4H); ^{13}C NMR (75 MHz, $CDCl_3$) δ 152.7, 149.6, 145.6, 135.7, 133.4, 130.2, 129.6, 127.9, 127.7, 126.0, 125.4 (2C), 120.1, 114.5, 114.0, 113.9, 113.8, 107.4, 62.7, 53.5, 45.3; ESI-MS *m/z* 412 [*M*+H]$^+$.

4-((7-Fluoropyrrolo[1,2-*a*]quinoxalin-4-yl)methyl)piperazin-1-yl)(1*H*-1,2,4-triazol-1-yl)methanone (5i). Starting from **12a** (15 mg, 0.08 mmol) and **14e** (14 mg, 0.08 mmol), title compound was prepared according to the procedure previously described for **5a**. Silica gel column chromatography (EtOAc) provided pure compound (25% yield) as a colourless oil; ^{1}H NMR (300 MHz, $CDCl_3$) δ 8.78 (s, 1H), 7.97 (s, 1H), 7.90 (s, 1H), 7.81 (dd, *J* = 9.0, 5.0 Hz, 1H), 7.65 (dd, *J* = 9.5, 2.6 Hz, 1H), 7.32-7.18 (m, 1H), 7.15 (d, *J* = 3.9 Hz, 1H), 6.91-6.82 (m, 1H), 3.94 (m, 6H), 2.76 (m, 4H); ^{13}C NMR (75 MHz, $CDCl_3$) δ 160.0 (d, J_{C-F} = 243.8 Hz), 153.9, 152.2, 148.7, 146.9, 136.9 (d, J_{C-F} = 11.4 Hz), 125.8, 124.4 (d, J_{C-F} = 1.9 Hz), 115.7 (d, J_{C-F} = 10.2 Hz), 115.4 (d, J_{C-F} = 8.2 Hz), 115.0 (d, J_{C-F} = 9.2 Hz), 114.7, 114.1, 107.7, 62.5, 53.4, 47.1; ^{19}F NMR (282 MHz, $CDCl_3$) δ -116.9; ESI-MS *m/z* 380 [*M*+H]$^+$.

(1*H*-Benzo[*d*][1,2,3]triazol-1-yl)(4-((7-fluoropyrrolo[1,2-*a*]quinoxalin-4-yl)methyl)piperazin-1-yl)methanone (5j). Starting from **12a** (40.0 mg, 0.18 mmol) and **14h** (42 mg, 0.18 mmol), title compound was prepared according to the procedure previously described for **5a**. Silica gel column chromatography (PetEt/EtOAc 2:1) provided pure compound (28% yield) as a colourless oil; ^{1}H NMR (300 MHz, $CDCl_3$) δ 8.08 (d, *J* = 8.2 Hz, 1H), 7.99 (d, *J* = 8.3 Hz, 1H), 7.91 (s, 1H), 7.82 (dd, *J* = 9.0, 5.1 Hz, 1H), 7.71-7.54 (m, 2H), 7.50-7.39 (m, 1H), 7.30-7.22 (m, 1H), 7.18 (d, *J* = 3.9 Hz, 1H), 6.92-6.85 (m, 1H), 3.99 (m, 6H), 2.85 (m, 4H); ^{13}C NMR (75 MHz, $CDCl_3$) δ 158.1 (d, J_{C-F} = 244.1 Hz), 147.7, 146.6, 143.6, 135.0 (d, J_{C-F} = 11.6 Hz), 131.5, 127.7, 123.9, 123.5, 122.5 (d, J_{C-F} = 2.1 Hz), 118.2, 113.9 (d, J_{C-F} = 8.2 Hz), 113.5 (d, J_{C-F} = 6.3 Hz), 113.1 (d, J_{C-F} = 9.4 Hz), 112.8, 112.2, 111.9, 105.9, 60.6, 58.7, 51.6; ^{19}F NMR (282 MHz, $CDCl_3$) δ -117.0; ESI-MS *m/z* 430 [*M*+H]$^+$.

(4-((7-Chloropyrrolo[1,2-*a*]quinoxalin-4-yl)methyl)piperazin-1-yl)(1*H*-1,2,4-triazol-1-yl)methanone (5k). Starting from **12c** (25 mg, 0.11 mmol) and **14e** (20 mg, 0.11 mmol), title compound was prepared according to the procedure previously described for **5a**. Silica gel column chromatography (DCM/Acetone 9:1) provided pure compound (30% yield) as a colourless oil; ^{1}H NMR (300 MHz, $CDCl_3$) δ 8.79 (s, 1H), 7.97 (d, *J* = 3.9 Hz, 2H), 7.91 (d, *J* = 1.4 Hz, 1H), 7.79 (d, *J* = 8.8 Hz, 1H), 7.47 (dd, *J* = 8.8, 2.2 Hz, 1H), 7.16 (d, *J* = 4.0 Hz, 1H), 6.93-6.85 (m, 1H), 3.95 (m, 6H), 2.78 (m, 4H); ^{13}C NMR (75 MHz, $CDCl_3$) δ 155.2, 149.6, 145.5, 136.6, 133.3, 129.3, 127.6, 126.4, 125.5, 125.0, 115.1, 114.4, 113.7, 106.4, 60.21, 54.47, 53.40; ESI-MS *m/z*: 396 [*M*+H]$^+$.

(1*H*-Benzo[*d*][1,2,3]triazol-1-yl)(4-((7-chloropyrrolo[1,2-*a*]quinoxalin-4-yl)methyl)piperazin-1-yl)methanone (5l). Starting from **12c** (30 mg, 0.13 mmol) and **14h** (30 mg, 0.13 mmol), title compound was prepared according to the procedure previously described for **5a**. Silica gel column chromatography (PetEt/EtOAc 9:1) provided pure compound (32% yield) as a colourless oil; ^{1}H NMR (300 MHz, $CDCl_3$) δ 8.09 (d, *J* = 7.6 Hz, 1H), 8.02-7.95 (m, 2H), 7.91 (s, 1H), 7.79 (d, *J* = 8.8 Hz, 1H), 7.60 (t, *J* = 7.7 Hz, 1H), 7.46 (dt, *J* = 15.4, 5.4 Hz, 2H), 7.19 (d, *J* = 4.0 Hz, 1H), 6.94-6.86 (m, 1H), 3.99 (m, 6H), 2.85 (m, 4H); ^{13}C NMR (75 MHz, $CDCl_3$) δ 153.9, 149.6, 145.6, 136.7, 133.4, 130.5, 129.7, 129.6, 127.9, 126.3, 125.9, 125.5, 120.1, 115.0, 114.9, 114.4, 113.8, 107.9, 62.4, 53.5, 53.4; ESI-MS *m/z*: 446 [*M*+H]$^+$.

(4-((7,8-Dimethylpyrrolo[1,2-*a*]quinoxalin-4-yl)methyl)piperazin-1-yl)(1*H*-1,2,4-triazol-1-yl)methanone (5m). Starting from **12d** (75 mg, 0.33 mmol) and **14e** (60 mg, 0.33 mmol), title compound was prepared according to the procedure previously described for **5a**. Silica gel column chromatography (EtOAc) provided pure compound (35% yield) as a colourless oil; ^{1}H NMR (300 MHz, $CDCl_3$) δ 8.78 (s, 1H), 7.97 (s, 1H), 7.88 (d, *J* = 1.3 Hz, 1H), 7.75 (s, 1H), 7.62 (s, 1H), 7.10 (d, *J* = 4.0 Hz, 1H), 6.88-6.76 (m, 1H), 3.94 (m, 6H), 2.76 (m, 4H), 2.45 (s, 3H), 2.39 (s, 3H); ^{13}C NMR (75 MHz, $CDCl_3$) δ 152.2, 151.5, 148.7, 146.8, 137.5, 134.3, 133.7, 130.2, 126.1, 125.6, 114.3, 114.0, 113.6, 106.8, 62.6, 53.4, 53.2, 20.5, 19.8; ESI-MS *m/z*: 390 [*M*+H]$^+$.

(1*H*-Benzo[*d*][1,2,3]triazol-1-yl)(4-((7,8-dimethylpyrrolo[1,2-*a*]quinoxalin-4-yl)methyl) piperazin-1-yl)methanone (5n). Starting from **12d** (48 mg, 0.21 mmol) and **14h** (50 mg, 0.21 mmol), title compound was prepared according to the procedure previously described for **5a**. Silica gel column chromatography (PetEt/EtOAc 2:1) provided pure compound (26% yield) as a yellow solid; ^{1}H NMR (300 MHz, $CDCl_3$) δ 8.08 (d, *J* = 8.3 Hz, 1H), 8.02-7.95 (m, 1H), 7.90-7.86 (m, 1H), 7.75 (s, 1H), 7.62 (s, 1H), 7.60-7.56 (m, 1H), 7.49-7.39 (m, 1H), 7.12 (d, *J* = 4.0 Hz, 1H), 6.88-6.82 (m, 1H), 3.97 (m, 6H), 2.83 (m, 4H), 2.45 (s, 3H), 2.39 (s, 3H). ^{13}C NMR (75 MHz, $CDCl_3$) δ 151.6, 149.6, 145.5, 137.4, 134.2, 133.9, 133.4, 130.3, 129.5, 126.1, 125.7, 125.4, 120.1, 114.3, 114.0, 113.8, 113.6, 106.8, 62.7, 53.5, 53.4, 20.5, 19.8; ESI-MS *m/z* 440 [*M*+H]$^+$.

(1*H*-Benzo[*d*][1,2,3]triazol-1-yl)(4-(((7-fluoropyrrolo[1,2-*a*]quinoxalin-4-yl)methyl)amino) piperidin-1-yl)methanone (6a). Starting from **12a** (40 mg, 0.18 mmol) and **16** (45 mg, 0.18 mmol), title compound was prepared according to the procedure previously described for **5a**. Silica gel column chromatography (EtOAc) provided pure compound (30% yield) as a yellow solid; ^{1}H NMR (300 MHz, $CDCl_3$) δ 8.09 (d, *J* = 7.0 Hz, 1H), 7.98 (d, *J* = 8.3 Hz, 1H), 7.93-7.89 (m, 1H), 7.82 (dd, *J* = 9.0, 5.0 Hz, 1H), 7.68-7.55 (m, 2H), 7.45 (t, *J* = 7.7 Hz, 1H), 7.25 (dd, *J* = 17.0, 2.8 Hz, 1H), 6.95 (d, *J* = 2.8 Hz, 1H), 6.90-6.85 (m, 1H), 4.69 (br s, 1H), 4.46 (d, *J* = 13.4 Hz, 2H), 4.26 (s, 2H), 3.40 (t, *J* = 12.1 Hz, 2H), 3.16-3.00 (m, 1H), 2.29-2.10 (m, 2H), 1.90-1.69 (m, 2H); ^{13}C NMR (75 MHz, $CDCl_3$) δ 158.1 (d, J_{C-F} = 244.1 Hz), 152.0, 147.7, 143.7, 135.0 (d, J_{C-F} = 11.6 Hz), 131.5, 127.7, 123.9, 123.5, 122.5 (d, J_{C-F} = 2.1 Hz), 118.2, 113.9 (d, J_{C-F} = 8.2 Hz), 113.5 (d, J_{C-F} = 6.3 Hz), 113.1 (d, J_{C-F} = 9.4 Hz), 112.8, 112.2, 111.9, 105.8, 60.6, 58.7, 51.7, 51.6; ^{19}F NMR (282 MHz, $CDCl_3$) δ -117.0; ESI-MS *m/z* 444 [*M*+H]$^+$.

(1*H*-Benzo[*d*][1,2,3]triazol-1-yl)(4-(((7-chloropyrrolo[1,2-*a*]quinoxalin-4-yl)methyl)amino) piperidin-1-yl)methanone (6b). Starting from **12c** (30 mg, 0.13 mmol) and **16** (32 mg, 0.13 mmol), title compound was prepared according to the procedure previously described for **5a**. Silica gel column chromatography (PetEt/EtOAc 1:1) provided pure compound (33% yield) as a yellow solid; ^{1}H NMR

View Article Online
DOI: 10.1039/C6RA12524G

(300 MHz, $CDCl_3$) δ 8.09 (d, *J* = 8.3 Hz, 1H), 8.01-7.87 (m, 3H), 7.78 (d, *J* = 8.8 Hz, 1H), 7.60 (t, *J* = 7.7 Hz, 1H), 7.46 (dd, *J* = 12.9, 4.7 Hz, 2H), 6.96 (d, *J* = 4.0 Hz, 1H), 6.92-6.86 (m, 1H), 4.45 (d, *J* = 13.2 Hz, 2H), 4.24 (s, 2H), 3.46-3.34 (m, 2H), 3.08-3.01 (m, 1H), 2.17 (m, 3H), 1.86-1.74 (m, 2H). ^{13}C NMR (75 MHz, $CDCl_3$) δ 155.2, 149.6, 145.6, 136.6, 133.7, 133.4, 130.5, 129.5, 129.4, 127.7, 126.3, 125.4, 125.1, 120.0, 115.2, 115.1, 114.4, 113.7, 106.4, 60.6, 54.5, 53.6, 49.2; ESI-MS *m/z* 460 $[M+H]^+$.

(1*H*-Benzo[*d*][1,2,3]triazol-1-yl)(4-(((7,8-dimethylpyrrolo[1,2-*a*]quinoxalin-4-yl)methyl)amino)piperidin-1-yl)methanone (6c). Starting from **12d** (55 mg, 0.24 mmol) and **16** (60 mg, 0.24 mmol), title compound was prepared according to the procedure previously described for **5a**. Silica gel column chromatography (EtOAc) provided pure compound (28% yield) as a yellow solid; ^1H NMR (300 MHz, $CDCl_3$) δ 8.09 (d, *J* = 8.3 Hz, 1H), 7.97 (d, *J* = 8.3 Hz, 1H), 7.88 (d, *J* = 1.4 Hz, 1H), 7.71 (s, 1H), 7.65-7.55 (m, 2H), 7.45 (t, *J* = 7.7 Hz, 1H), 6.86 (dt, *J* = 15.5, 3.4 Hz, 2H), 4.44 (d, *J* = 13.4 Hz, 2H), 4.22 (s, 2H), 3.49 - 3.46 (m, 2H), 3.15-2.94 (m, 1H), 2.45 (s, 3H), 2.40 (s, 3H), 2.16-2.06 (m, 3H), 1-83-1.70 (m, 2H); ESI-MS *m/z* 454 $[M+H]^+$.

Molecular Modelling studies

Molecular Docking

a) Ligand preparation

Three-dimensional structures of all compounds in this study were built by means of Maestro (Maestro, version 9.3, Schrödinger, LLC, New York, NY, 2012). Molecular energy minimizations were performed by means of MacroModel (MacroModel, version 9.9, Schrödinger, LLC, New York, NY, 2012) using the Optimized Potentials for Liquid Simulations-all atom (OPLS-AA) force field 2005.[48] The solvent effects are simulated using the analytical Generalized-Born/Surface-Area (GB/SA) model,[49] and no cutoff for nonbonded interactions was selected. Polak-Ribiere conjugate gradient (PRCG) method with 1000 maximum iterations and 0.001 gradient convergence threshold was employed. All compounds reported in this paper were treated by LigPrep application (LigPrep, version 2.5, Schrödinger, LLC, New York, NY, 2012), implemented in Maestro suite 2011, generating the most probable ionization state of any possible enantiomers and tautomers at cellular pH value (7 ± 0.5). QikProp (QikProp, version 3.5; Schrödinger, LLC: New York, 2012) was used to assess the physico-chemical properties of selected compounds. The output is reported in Supplementary Information in Table S1.

b) Protein preparation

The three-dimensional structures of FAAH (PDB ID: 3PPM[50]) and MAGL enzymes (PDB ID: 3HJU[11]) were taken from PDB and imported into Schrödinger Maestro molecular modeling environment. Water molecules, compounds used for the crystallization and the co-crystallized ligand were removed from the available experimental structures. The obtained enzymes were submitted to protein preparation wizard implemented in Maestro suite 2012 as described by us.[51-53] This protocol through a series of computational steps, allowed us to obtain a reasonable starting structure of the proteins for molecular docking calculations by a series of computational steps. In particular, we performed three steps to (1) add hydrogens, (2) optimize the orientation of hydroxyl groups, Asn, and Gln, and the protonation state of His, and (3) perform a constrained refinement with the impref utility, setting the max RMSD of 0.30. The impref utility consists of a cycles of energy minimization based on the impact molecular mechanics engine and on the OPLS_2005 force field.[48]

c) Molecular Docking

Molecular docking was carried out using the Schrödinger suite 2011 by applying the IFD protocol (Schrödinger Suite 2012 Induced Fit Docking protocol; Glide version 5.8, Schrödinger, LLC, New York, NY, 2012; Prime version 3.1, Schrödinger, LLC, New York, NY, 2012). This procedure induces conformational changes in the binding site to accommodate the ligand and exhaustively identify possible binding modes and associated conformational changes by side-chain sampling and backbone minimization. The proteins and the ligands used were prepared as reported in the previous paragraphs. The boxes for docking calculation were built taking into account the centroid of the co-crystallized ligand for FAAH enzyme, while for MAGL enzyme the catalytic serine 122, employing default setting. IFD includes protein side-chain flexibility in a radius of 5.0 Å around the poses found during the initial docking stage of the IFD protocol. Complexes within 30.0 kcal/mol of minimum energy structure were taken forward for redocking. The Glide redocking stage was performed by XP (Extra Precision) methods. No hydrogen bonding or other constraints were used. Hydrophobic contacts for the described ligand/protein complexes were visualized by using the python script "*display_hydrophobic_interactions.py*" implemented in Maestro suite.

Enzyme assays

MAGL and FAAH activities were detected in COS cells and rat brain, respectively. In particular, 2-AG hydrolysis was measured by incubating the 10,000xg cytosolic fraction of either COS cells or rat brain homogenate (100 μg/sample) in Tris–HCl 50 mM, at pH 7.4 at 37 °C for 20 min, with synthetic 2-arachidonoyl-[^3H]-glycerol (40 Ci/mmol, ARC St. Louis, MO, USA) properly diluted with 2-AG (Cayman Chemicals, Ann Arbor, MI, USA). After incubation, the amount of [^3H]-glycerol produced was measured by scintillation counting of the aqueous phase after extraction of the incubation mixture with 2 volumes of $CHCl_3$/MeOH 1:1 (by vol.). For time-course experiments, the effect of compounds on MGL activity was measured after 10 min and 60 min of pre-incubation with the enzyme followed by a 20 min of incubation with the specific substrate. AEA hydrolysis was measured by incubating the 10,000xg membrane fraction of rat brain (70 μg/sample) in Tris–HCl 50 mM, at pH 9.5 at 37 °C for 30 min, with synthetic *N*-arachidonoyl-[^{14}C]-ethanolamine (110 mCi/mmol, ARC St. Louis, MO, USA) properly diluted with AEA (Tocris Bioscience, Avonmouth, Bristol, UK). After incubation, the amount of [^{14}C]-ethanolamine produced was measured by scintillation counting of the aqueous phase after extraction of the incubation mixture with 2 volumes of $CHCl_3$/MeOH 1:1 (by vol.).

View Article Online
DOI: 10.1039/C6RA12524G

Conclusions

In conclusion, we described herein the identification of novel FAAH and MAGL inhibitors characterized by a pyrroloquinoxaline-based structure. Among the newly synthesized chemical entities, compounds **5e**, **5i**, **5k** and **5m** showed relatively high potency on both target enzymes and favorable predicted drug-like properties, thus fostering further investigation and optimization for this novel class of dual endocannabinoid metabolizing enzyme inhibitors. Moreover we gained insights into the molecular determinants for specific enzyme inhibition.

Acknowledgements

PRIN-Miur is kindly acknowledged.

Notes and references

1. K. Mackie, *J Neuroendocrinol*, 2008, **20 Suppl 1**, 10-14.

2. B. F. Cravatt and A. H. Lichtman, *J Neurobiol*, 2004, **61**, 149-160.

3. V. Di Marzo and S. Petrosino, *Curr. Opin. Lipidol.*, 2007, **18**, 129-140.

4. M. N. Hill and B. B. Gorzalka, *CNS Neurol Disord Drug Targets*, 2009, **8**, 451-458.

5. S. Petrosino and V. Di Marzo, *Curr Opin Investig Drugs*, 2010, **11**, 51-62.

6. F. Piscitelli and V. Di Marzo, *ACS Chem Neurosci*, 2012, **3**, 356-363.

7. J. R. Savinainen, S. M. Saario and J. T. Laitinen, *Acta Physiol (Oxf)*, 2012, **204**, 267-276.

8. F. Fezza, C. De Simone, D. Amadio and M. Maccarrone, *Subcell Biochem*, 2008, **49**, 101-132.

9. M. Maccarrone, E. Dainese and S. Oddi, *Trends Biochem Sci*, 2010, **35**, 601-608.

10. M. H. Bracey, M. A. Hanson, K. R. Masuda, R. C. Stevens and B. F. Cravatt, *Science*, 2002, **298**, 1793-1796.

11. G. Labar, C. Bauvois, F. Borel, J. L. Ferrer, J. Wouters and D. M. Lambert, *Chembiochem*, 2010, **11**, 218-227.

12. S. G. Kinsey, J. Z. Long, B. F. Cravatt and A. H. Lichtman, *J Pain*, 2010, **11**, 1420-1428.

13. M. N. Hill, C. J. Hillard, F. R. Bambico, S. Patel, B. B. Gorzalka and G. Gobbi, *Trends Pharmacol Sci*, 2009, **30**, 484-493.

14. V. Di Marzo, N. Stella and A. Zimmer, *Nat Rev Neurosci*, 2015, **16**, 30-42.

15. S. M. Saario, J. R. Savinainen, J. T. Laitinen, T. Jarvinen and R. Niemi, *Biochem Pharmacol*, 2004, **67**, 1381-1387.

16. K. Otrubova, C. Ezzili and D. L. Boger, *Bioorg Med Chem Lett*, 2011, **21**, 4674-4685.

17. K. Ahn, D. S. Johnson, L. R. Fitzgerald, M. Liimatta, A. Arendse, T. Stevenson, E. T. Lund, R. A. Nugent, T. K. Nomanbhoy, J. P. Alexander and B. F. Cravatt, *Biochemistry*, 2007, **46**, 13019-13030.

18. J. M. Keith, R. Apodaca, W. Xiao, M. Seierstad, K. Pattabiraman, J. Wu, M. Webb, M. J. Karbarz, S. Brown, S. Wilson, B. Scott, C. S. Tham, L. Luo, J. Palmer, M. Wennerholm, S. Chaplan and J. G. Breitenbucher, *Bioorg Med Chem Lett*, 2008, **18**, 4838-4843.

19. J. Z. Long, W. Li, L. Booker, J. J. Burston, S. G. Kinsey, J. E. Schlosburg, F. J. Pavon, A. M. Serrano, D. E. Selley, L. H. Parsons, A. H. Lichtman and B. F. Cravatt, *Nat Chem Biol*, 2009, **5**, 37-44.

20. J. W. Chang, M. J. Niphakis, K. M. Lum, A. B. Cognetta, 3rd, C. Wang, M. L. Matthews, S. Niessen, M. W. Buczynski, L. H. Parsons and B. F. Cravatt, *Chem Biol*, 2012, **19**, 579-588.

21. J. Z. Long, D. K. Nomura, R. E. Vann, D. M. Walentiny, L. Booker, X. Jin, J. J. Burston, L. J. Sim-Selley, A. H. Lichtman, J. L. Wiley and B. F. Cravatt, *Proc Natl Acad Sci U S A*, 2009, **106**, 20270-20275.

22. N. Aaltonen, J. R. Savinainen, C. R. Ribas, J. Ronkko, A. Kuusisto, J. Korhonen, D. Navia-Paldanius, J. Hayrinen, P. Takabe, H. Kasnanen, T. Pantsar, T. Laitinen, M. Lehtonen, S. Pasonen-Seppanen, A. Poso, T. Nevalainen and J. T. Laitinen, *Chem Biol*, 2013, **20**, 379-390.

23. S. Butini, M. Brindisi, S. Gemma, P. Minetti, W. Cabri, G. Gallo, S. Vincenti, E. Talamonti, F. Borsini, A. Caprioli, M. A. Stasi, S. Di Serio, S. Ros, G. Borrelli, S. Maramai, F. Fezza, G. Campiani and M. Maccarrone, *J Med Chem*, 2012, **55**, 6898-6915.

24. S. Butini, S. Gemma, M. Brindisi, S. Maramai, P. Minetti, D. Celona, R. Napolitano, F. Borsini, W. Cabri, F. Fezza, L. Merlini, S. Dallavalle, G. Campiani and M. Maccarrone, *Bioorg Med Chem Lett*, 2013, **23**, 492-495.

View Article Online
DOI: 10.1039/C6RA12524G

25. M. Brindisi, S. Maramai, S. Gemma, S. Brogi, A. Grillo, L. Di Cesare Mannelli, E. Gabellieri, S. Lamponi, S. Saponara, B. Gorelli, D. Tedesco, T. Bonfiglio, C. Landry, K. M. Jung, A. Armirotti, L. Luongo, A. Ligresti, F. Piscitelli, C. Bertucci, M. P. Dehouck, G. Campiani, S. Maione, C. Ghelardini, A. Pittaluga, D. Piomelli, V. Di Marzo and S. Butini, *J Med Chem*, 2016, **59**, 2612-2632.

26. J. Lim, M. Igarashi, K. M. Jung, S. Butini, G. Campiani and D. Piomelli, *Neuropsychopharmacology*, 2016, **41**, 1329-1339.

27. D. Ramesh, T. F. Gamage, T. Vanuytsel, R. A. Owens, R. A. Abdullah, M. J. Niphakis, T. Shea-Donohue, B. F. Cravatt and A. H. Lichtman, *Neuropsychopharmacology*, 2013, **38**, 1039-1049.

28. A. Seillier, D. Dominguez Aguilar and A. Giuffrida, *Pharmacol Biochem Behav*, 2014, **124**, 153-159.

29. S. Ghosh, S. G. Kinsey, Q. S. Liu, L. Hruba, L. R. McMahon, T. W. Grim, C. R. Merritt, L. E. Wise, R. A. Abdullah, D. E. Selley, L. J. Sim-Selley, B. F. Cravatt and A. H. Lichtman, *J Pharmacol Exp Ther*, 2015, **354**, 111-120.

30. N. S. Adamson Barnes, V. A. Mitchell, N. P. Kazantzis and C. W. Vaughan, *Br J Pharmacol*, 2016, **173**, 77-87.

31. V. Naidoo, D. A. Karanian, S. K. Vadivel, J. R. Locklear, J. T. Wood, M. Nasr, P. M. Quizon, E. E. Graves, V. Shukla, A. Makriyannis and B. A. Bahr, *Neurotherapeutics*, 2012, **9**, 801-813.

32. B. A. Bahr, D. A. Karanian, S. S. Makanji and A. Makriyannis, *Expert Opin Investig Drugs*, 2006, **15**, 351-365.

33. A. Busquets-Garcia, E. Puighermanal, A. Pastor, R. de la Torre, R. Maldonado and A. Ozaita, *Biol Psychiatry*, 2011, **70**, 479-486.

34. S. P. Alexander and D. A. Kendall, *Br J Pharmacol*, 2007, **152**, 602-623.

35. S. Gemma, L. Colombo, G. Forloni, L. Savini, C. Fracasso, S. Caccia, M. Salmona, M. Brindisi, B. P. Joshi, P. Tripaldi, G. Giorgi, O. Taglialatela-Scafati, E. Novellino, I. Fiorini, G. Campiani and S. Butini, *Org Biomol Chem*, 2011, **9**, 5137-5148.

36. E. Morelli, S. Gemma, R. Budriesi, G. Campiani, E. Novellino, C. Fattorusso, B. Catalanotti, S. S. Coccone, S. Ros, G. Borrelli, M. Persico, I. Fiorini, V. Nacci, P. Ioan, A. Chiarini, M. Hamon, A. Cagnotto, T. Mennini, C. Fracasso, M. Colovic, S. Caccia and S. Butini, *J Med Chem*, 2009, **52**, 3548-3562.

37. G. Campiani, E. Morelli, S. Gemma, V. Nacci, S. Butini, M. Hamon, E. Novellino, G. Greco, A. Cagnotto, M. Goegan, L. Cervo, F. Dalla Valle, C. Fracasso, S. Caccia and T. Mennini, *J Med Chem*, 1999, **42**, 4362-4379.

38. G. Campiani, A. Cappelli, V. Nacci, M. Anzini, S. Vomero, M. Hamon, A. Cagnotto, C. Fracasso, C. Uboldi, S. Caccia, S. Consolo and T. Mennini, *J Med Chem*, 1997, **40**, 3670-3678.

39. S. Butini, R. Budriesi, M. Hamon, E. Morelli, S. Gemma, M. Brindisi, G. Borrelli, E. Novellino, I. Fiorini, P. Ioan, A. Chiarini, A. Cagnotto, T. Mennini, C. Fracasso, S. Caccia and G. Campiani, *J Med Chem*, 2009, **52**, 6946-6950.

40. B. B. Lv W., Pawlowski M., Connell P.P., Kozikowski A.P., *J. Med. Chem.*, 2016, DOI: 10.1021/acs.jmedchem.1025b01762.

41. V. Desplat, S. Moreau, A. Gay, S. B. Fabre, D. Thiolat, S. Massip, G. Macky, F. Godde, D. Mossalayi, C. Jarry and J. Guillon, *J Enzyme Inhib Med Chem*, 2010, **25**, 204-215.

42. J. Guillon, R. C. Reynolds, J. M. Leger, M. A. Guie, S. Massip, P. Dallemagne and C. Jarry, *J Enzyme Inhib Med Chem*, 2004, **19**, 489-495.

43. A. K. Ghosh and M. Brindisi, *J Med Chem*, 2015, **58**, 2895-2940.

44. J. Guillon, I. Forfar, M. Mamani-Matsuda, V. Desplat, M. Saliege, D. Thiolat, S. Massip, A. Tabourier, J. M. Leger, B. Dufaure, G. Haumont, C. Jarry and D. Mossalayi, *Bioorg Med Chem*, 2007, **15**, 194-210.

45. M. Y. Wu, G. Esteban, S. Brogi, M. Shionoya, L. Wang, G. Campiani, M. Unzeta, T. Inokuchi, S. Butini and J. Marco-Contelles, *Eur J Med Chem*, 2015.

46. S. Butini, S. Gemma, M. Brindisi, S. Maramai, P. Minetti, D. Celona, R. Napolitano, F. Borsini, W. Cabri, F. Fezza, L. Merlini, S. Dallavalle, G. Campiani and M. MacCarrone, *Bioorganic and Medicinal Chemistry Letters*, 2013, **23**, 492-495.

47. M. Chioua, M. Perez, O. M. Bautista-Aguilera, M. Yanez, M. G. Lopez, A. Romero, R. Cacabelos, R. P. de la Bellacasa, S. Brogi, S. Butini, J. I. Borrell and J. Marco-Contelles, *Mini reviews in medicinal chemistry*, 2015, **15**, 648-658.

48. W. L. Jorgensen, D. S. Maxwell and J. TiradoRives, *J. Am. Chem. Soc.*, 1996, **118**, 11225-11236.

49. W. C. Still, A. Tempczyk, R. C. Hawley and T. Hendrickson, *J. Am. Chem. Soc.*, 1990, **112**, 6127-6129.

View Article Online
DOI: 10.1039/C6RA12524G

50. M. Mileni, J. Garfunkle, C. Ezzili, B. F. Cravatt, R. C. Stevens and D. L. Boger, *J Am Chem Soc*, 2011, **133**, 4092-4100.

51. S. Brogi, S. Butini, S. Maramai, R. Colombo, L. Verga, C. Lanni, E. De Lorenzi, S. Lamponi, M. Andreassi, M. Bartolini, V. Andrisano, E. Novellino, G. Campiani, M. Brindisi and S. Gemma, *CNS Neurosci. Ther.*, 2014, **20**, 624-632.

52. M. Brindisi, S. Brogi, N. Relitti, A. Vallone, S. Butini, S. Gemma, E. Novellino, G. Colotti, G. Angiulli, F. Di Chiaro, A. Fiorillo, A. Ilari and G. Campiani, *Sci. Rep.*, 2015, **5**, 9705.

53. M. Brindisi, S. Gemma, S. Kunjir, L. Di Cerbo, S. Brogi, S. Parapini, S. D'Alessandro, D. Taramelli, A. Habluetzel, S. Tapanelli, S. Lamponi, E. Novellino, G. Campiani and S. Butini, *Med. Chem. Commun.*, 2015, **6**, 357-362.

View Article Online
DOI: 10.1039/C6RA12524G

Harnessing the pyrroloquinoxaline scaffold for FAAH and MAGL interaction: definition of the structural determinants for enzyme inhibition

Margherita Brindisi, Simone Brogi, Samuele Maramai, Alessandro Grillo, Giuseppe Borrelli, Stefania Butini,* Ettore Novellino, Marco Allarà, Alessia Ligresti, Giuseppe Campiani,* Vincenzo Di Marzo, Sandra Gemma